Frey, F.A., Coffin, M.F., Wallace, P.J., and Quilty, P.G. (Eds.)
Proceedings of the Ocean Drilling Program, Scientific Results Volume 183

Leg 183 Synthesis: Kerguelen Plateau–Broken Ridge—A Large Igneous Province[1]

F.A. Frey,[2] M.F. Coffin,[3,4] P.J. Wallace,[5] and D. Weis[6,7]

ABSTRACT

The Kerguelen Plateau and Broken Ridge form a large igneous province (LIP) in the southern Indian Ocean. The main objectives of Ocean Drilling Program Leg 183 were to understand the origin and evolution of this LIP and the impact of its formation on the environment. Igneous basement (33 to 233 m of penetration) has been recovered from 11 drill sites on the LIP, and 7 are Leg 183 sites. Studies of the basement and sediment cores lead to the following conclusions.

1. Formation of the LIP postdated breakup between India and Antarctica, with eruption ages ($^{40}Ar/^{39}Ar$) ranging from ~119 Ma in the southern Kerguelen Plateau (SKP) to ~34 Ma in the northern Kerguelen Plateau. Apparently, peaks in magmatic output (~0.9 km^3/yr) occurred in the intervals of 119–110 and 105–95 Ma. Although an important caveat is that we have access only to uppermost basement of a thick (~20 km) igneous crust, these results are inconsistent with massive volcanism associated with a single plume head and continental breakup.
2. The uppermost igneous basement is dominantly tholeiitic basalt. Based on the physical characteristics of the lava flows, which indicate subaerial eruption, and the occurrence of overlying terrestrially derived sediments containing wood fragments, fern remains, and terrestrial palynoflora, much of the LIP was above sea level when magmatic output was high.
3. The geochemical characteristics of basalt forming the LIP are unlike mid-ocean-ridge basalt (MORB). There are, however,

[1]Frey, F.A., Coffin, M.F., Wallace, P.J., and Weis, D., 2003. Leg 183 synthesis: Kerguelen Plateau–Broken Ridge—a large igneous province. *In* Frey, F.A., Coffin, M.F., Wallace, P.J., and Quilty, P.G. (Eds.), *Proc. ODP, Sci. Results,* 183, 1–48 [Online]. Available from World Wide Web: <http://www-odp.tamu.edu/publications/183_SR/VOLUME/SYNTH/SYNTH.PDF>. [Cited YYYY-MM-DD]
[2]Department of Earth, Atmospheric, and Planetary Sciences, Massachusetts Institute of Technology, Cambridge MA 02139, USA. fafrey@mit.edu
[3]Ocean Research Institute, University of Tokyo, 1-15-1 Minamidai, Nakano-ku, Tokyo 164-8639, Japan.
[4]Institute for Geophysics, Jackson School of Geosciences, The University of Texas at Austin, 4412 Spicewood Springs Road, Austin TX 78759-8500, USA.
[5]Ocean Drilling Program, Texas A&M University, 1000 Discovery Drive, College Station TX 77845-9547, USA. Present address: Department of Geological Sciences, University of Oregon, Eugene OR 97403-1272, USA.
[6]Department of Earth and Environmental Sciences–CP160/02, Université Libre de Bruxelles, Avenue F.D. Roosevelt, 50, 1050 Brussels, Belgium.
[7]Earth and Ocean Sciences, University of British Columbia, 6339 Stores Road, Vancouver BC V6T 1Z4, Canada.

Initial receipt: 22 April 2002
Acceptance: 16 December 2002
Web publication: 19 March 2003
Ms 183SR-015

significant geochemical differences between tholeiitic basalt erupted at each site. These differences are attributed to varying proportions of components derived from the Kerguelen plume, depleted MORB-related asthenosphere, and continental lithosphere.

4. Based on radiogenic isotopic ratios and incompatible element abundances, tholeiitic basalt of Cretaceous age from spatially diverse locations (Site 738 in the SKP, Site 1137 on Elan Bank, Site 747 in the Central Kerguelen Plateau (CKP), and Site 1142 on Broken Ridge) contains up to ~5% of a component derived from continental crust. The Proterozoic-age zircon and monazite in clasts of garnet-biotite gneiss in a conglomerate intercalated with basalt at Site 1137 demonstrate that continental crust fragments are present in the Indian Ocean lithosphere.
5. Surprising new results for oceanic LIPs are the dominance of alkalic lavas, trachybasalt to trachyte and rhyolite, at Skiff Bank and the pyroclastic deposits present on Skiff Bank, Elan Bank, and the CKP. Explosive subaerial volcanism at high latitudes can contribute volatiles to the stratosphere; therefore, LIP volcanism may have had a significant environmental impact.
6. Flora and fauna preserved in Kerguelen Plateau sediments provide a long-term record of the plateau's environment, beginning with terrestrial and shallow-marine deposition followed by equable Cretaceous paleoceanographic conditions, the abrupt Cretaceous/Tertiary boundary, the Late Paleocene Thermal Maximum, and cooling of the Southern Ocean through Tertiary time.

INTRODUCTION

Kerguelen Plateau and Broken Ridge (Fig. F1) form a large igneous province (LIP) that is interpreted to represent voluminous Cretaceous volcanism associated with arrival of the Kerguelen plume head below young Indian Ocean lithosphere (e.g., Morgan, 1981; Duncan and Storey, 1992; Storey, 1995). Subsequently, northward movement of the Indian plate over the plume stem formed a 5000-km-long, ~82- to 38-Ma hotspot track, the Ninetyeast Ridge (Duncan, 1991). At ~40 Ma, the westward-propagating Southeast Indian Ridge (SEIR) separated Broken Ridge from the Central Kerguelen Plateau (CKP) and the plume coincided with the ridge axis. As the SEIR migrated northeast relative to the plume, hotspot magmatism became confined to the Antarctic plate. From ~40 Ma to the present, the Kerguelen archipelago, Heard and McDonald Islands, and a northwest-southeast–trending chain of submarine volcanoes between these islands were constructed on the northern Kerguelen Plateau (NKP) and CKP (e.g., Weis et al., 2002). Thus, an ~120-m.y. record of volcanism is attributed to the Kerguelen plume (Fig. F1). The submarine basement of the LIP has been sampled at 11 Ocean Drilling Program (ODP) drill sites and that of the Ninetyeast Ridge has been sampled at 7 drill sites by ODP and the preceding Deep Sea Drilling Project (DSDP) (Figs. F1, F2).

F1. Basalt provinces in the eastern Indian Ocean, p. 36.

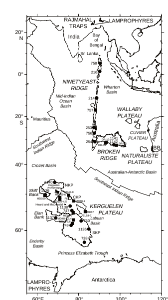

F2. Drill holes on the Kerguelen Plateau and Broken Ridge, p. 37.

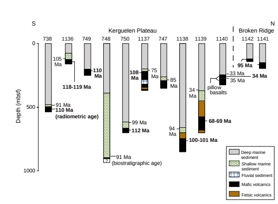

SCIENTIFIC OBJECTIVES

Leg 183 was the first Ocean Drilling Program leg dedicated to sampling the igneous basement of an oceanic plateau with the goals of understanding its origin and evolution. An overall objective of Leg 183 was to evaluate the hypothesis that the Kerguelen Plateau and Broken Ridge LIP formed as a result of volcanism associated with ascent of a plume head with subsequent volcanism resulting from the plume stem. To accomplish this objective, Leg 183 focused on three major problems related to the formation and evolution of the LIP:

1. Magmatic and tectonic development of the Kerguelen Plateau and Broken Ridge: we investigated how magma flux varied as a function of time to test the plume model for magma production rates during the formation of LIPs. We also examined relationships between magmatism and tectonism to understand how LIP development was related to the breakup of Gondwana and seafloor spreading.
2. Petrogenesis of basement igneous rocks: we sought to constrain the mineralogy and composition of the mantle sources that contributed to the magmatism, the melting processes that created the magmas, and the postmelting magmatic evolution. A specific objective was to evaluate the relative roles of a plume, asthenosphere, and continental lithosphere in the magmatism that formed the different domains of this LIP.
3. Environmental impact: what were the environmental effects of LIP magmatism? In particular, we sought to answer the following questions. During periods of high magma flux was it likely that (a) released volatiles and particulates affected the climate and (b) hydrothermal alteration affected the geochemical characteristics of seawater?

Important advances in solving these problems arose from shipboard observations that are summarized in Shipboard Scientific Party (2000) and Frey et al. (2000a). In this synthesis of postcruise results we summarize the progress made in addressing these three problems. Furthermore, we summarize advances in our understanding of Cretaceous and Cenozoic paleoenvironments and paleoceanography yielded by the sedimentary sections overlying igneous basement. The overall objectives and results of Leg 183 are complemented by ongoing studies of the Cenozoic subaerial lavas that form the Kerguelen archipelago (Damasceno et al., 2002; Doucet et al., 2002; Frey et al., 2002a; Mattielli et al., 2002).

CHRONOLOGY OF KERGUELEN PLATEAU AND BROKEN RIDGE MAGMATISM AND TECTONISM: IMPLICATIONS FOR THE PLUME HYPOTHESIS AND THE BREAKUP OF GONDWANA

Geochronology

High-quality radiometric age determinations are crucial for understanding the chronology and rates of Kerguelen hotspot magmatism, the dynamic mantle processes responsible for the magmatism, and temporal relationships between magmatism and potentially related environmental changes. Leg 183 added five sites to the preexisting four igneous basement drill sites on the Kerguelen Plateau and provided the first drilled basement samples from Broken Ridge. Basalt from 10 of the 11 drill sites on the two features has now yielded high-quality radiometric ($^{40}Ar/^{39}Ar$) ages (Fig. F2) (Whitechurch et al., 1992; Coffin et al., 2002; Duncan, 2002). Eruption ages are also available for other mafic lavas that have been attributed to the Kerguelen hotspot, that is, the Ninetyeast Ridge (Duncan, 1978, 1991), the Kerguelen archipelago (Nicolaysen et al., 2000), northeast India (Baksi, 1995; Coffin et al., 2002; Kent et al., 2002), southwest Australia (Frey et al., 1996; Coffin et al., 2002), and Antarctica (Coffin et al., 2002).

In general, ages young northward on the Kerguelen Plateau (Figs. F1, F2). On the southern Kerguelen Plateau (SKP), ages are 118–119 Ma (Site 1136), ~112 Ma (Site 750), and ~110 Ma (Site 749) (Whitechurch et al., 1992; Coffin et al., 2002; Duncan, 2002). Elan Bank yielded an age of 107–108 Ma (Site 1137), and the CKP 100–101 Ma (Site 1138) (Duncan, 2002). Broken Ridge, prior to Eocene breakup, abutted the CKP and has yielded ages of 94–95 Ma (Sites 1141 and 1142) (Duncan, 2002); younger ages reported for basalt dredged from Broken Ridge (Duncan, 1991) are not considered reliable because of alteration (loss of ^{40}Ar) (Duncan, pers. comm., 2002). The age of Skiff Bank is 68 to 69 Ma (Site 1139) (Duncan, 2002) and that of the northern NKP is 34 to 35 Ma (Site 1140) (Duncan, 2002). Age determinations for Ninetyeast Ridge basalt range from ~82 to ~38 Ma from north to south, respectively (Duncan, 1978, 1991). The Bunbury Basalt of southwest Australia (~123–132 Ma) (Frey et al., 1996; Coffin et al., 2002), the Rajmahal Traps of northeast India (~117–118 Ma) (Baksi, 1995; Coffin et al., 2002; Kent et al., 2002), and Indian and Antarctic lamprophyres (~115 and ~114 Ma, respectively) (Coffin et al., 2002) are believed to be continental expressions of the Kerguelen hotspot (Storey et al., 1992; Ingle et al., 2002b).

Kerguelen Hotspot Magma Flux

The radiometric age determinations described above have been combined with crustal volumes determined from wide-angle seismic data and gravity modeling to calculate the magma output rate of the Kerguelen hotspot through time (Fig. F3) (Coffin et al., 2002). Initial output rates were low from ~132 to ~123 Ma with eruption of the Bunbury Basalt. Between ~120 and ~110 Ma, rates increased by several orders of magnitude, to ~0.9 km^3/yr, with emplacement of the SKP, Rajmahal Traps, and lamprophyres on the Indian and Antarctic continental margins. Following this peak rate, output appears to have waned to ~0.1 km^3/yr for several million years, although this may be an artifact of sparse sampling or errors in assessing the contribution of hotspot magmatism to the crustal volume of Elan Bank. The CKP formed between ~105 and ~100 Ma at a rate of 0.9 km^3/yr, similar to that of the SKP. Next, Broken Ridge formed from ~100 to ~95 Ma at a slightly lower rate of 0.8 km^3/yr. Between ~120 and ~95 Ma, Kerguelen hotspot magma output rates exceed those of most known hotspot tracks (White, 1993), although an estimate of the magma flux during emplacement of the Ontong Java Plateau is an order of magnitude higher, at 8.9 km^3/yr (Eldholm and Coffin, 2000).

No rocks have been definitively identified as products of the Kerguelen hotspot between ~95 and ~82 Ma, although the oldest part of

F3. Estimated Kerguelen hotspot magma output since ≈130 Ma, p. 38.

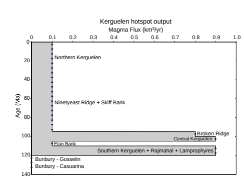

Ninetyeast Ridge, buried beneath the Bengal Fan, may have formed during this interval. Whether magma flux diminished abruptly or gradually by nearly an order of magnitude, to ~0.1 km³/yr between ~95 and ~82 Ma, is open to interpretation. Coffin et al. (2002) assumed an abrupt change at ~95 Ma. Between ~82 and ~38 Ma, the Kerguelen hotspot generated the Ninetyeast Ridge and Skiff Bank at a rate of ~0.1 km³/yr. Finally, from ~40 Ma to present, the hotspot has produced the NKP, including the Kerguelen archipelago and Heard and McDonald Islands, at about the same rate as during the ~82- to 38-Ma interval. Tertiary and Quaternary output rates of ~0.1 km³/yr for the Kerguelen hotspot are typical of many hotspots, including Hawaii (White, 1993). Since ~40 Ma, some changes in magma flux are suggested by a ~30- to 24-Ma episode of volcanism in the Kerguelen archipelago (Nicolaysen et al., 2000). Since ~130 Ma, ~2.5 × 10⁷ km³ of magma has been attributed to the Kerguelen hotspot. This estimate excludes normal thickness oceanic crust and volumes that contain dominantly continental material (Coffin et al., 2002). A previous estimate that also excluded normal thickness oceanic crust but did not subtract any continental crust was 75% larger, at 4.4 × 10⁷ km³ (Saunders et al., 1994).

The Kerguelen Hotspot and Indian Ocean Plate Reconstructions

Plate motions in the Indian Ocean region since ~130 Ma have resulted in both continental and oceanic lithosphere of variable thickness transiting over the Kerguelen hotspot's asthenospheric source region. Furthermore, paleolatitudes of Kerguelen Plateau and Ninetyeast Ridge rocks suggest 3°–10° of southward motion of the Kerguelen hotspot relative to the rotation axis since 100 Ma, a result that can be numerically modeled with large-scale mantle flow affecting the location of the plume conduit (Antretter et al., 2002). Plate reconstruction models for the Indian and Southern Oceans since 130 Ma (Coffin et al., 2002, without southward plume motion; Kent et al., 2002, with southward plume motion) indicate that seafloor spreading initiated between Western Australia and Greater India at ~133 Ma (Fig. F4). The age of initiation of seafloor spreading between India and Antarctica, however, is more problematic (e.g., Kent et al., 2002). Because of a lack of definitive geophysical or geological data, the initial age of continental breakup between India and Antarctica could be as young as ~132 Ma (e.g., Gaina et al., in press; Kent et al., 2002) or as old as ~165 Ma (e.g., Roeser et al., 1996). As described later, the presence of continental lithosphere within the Kerguelen Plateau (Elan Bank and SKP) and possibly Broken Ridge and of apparent oceanic crust in the Enderby Basin and Princess Elizabeth Trough between the Kerguelen Plateau and Antarctica (Fig. F1) indicates that when India and Antarctica first broke up, continental portions of Elan Bank and the SKP were attached to Greater India. Subsequently, at least portions of the Early Cretaceous mid-ocean-ridge system between Antarctica and India jumped northward toward India one or more times as the Enderby Basin continued to open, creating the Elan Bank microcontinent and dispersing continental fragments in the SKP (Coffin et al., 2002; Kent et al., 2002). One or more ridge jumps, in turn, suggest the existence of one or more abandoned Early Cretaceous spreading centers between Antarctica and the Kerguelen Plateau and that the Enderby Basin began opening prior to ~132 Ma. Uncertainties in the regional tectonic development make evaluation of the initial

F4. Plate reconstructions of the southern Indian Ocean, p. 39.

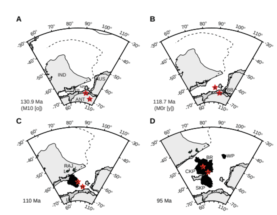

effects of various plume models, including impact and incubation, difficult, especially with respect to cause and effect of plume activity and continental breakup.

The first appearance of magmas possibly related to the Kerguelen hotspot, the Casuarina (~128–132 Ma) and Gosselin (~123 Ma) types of Bunbury Basalt in southwest Australia (Figs. F1, F4), correlates both temporally and spatially with continental breakup between Australia and Greater India and between Australia and Antarctica, respectively. Lower Cretaceous volcanic rock capping the Naturaliste Plateau (Figs. F1, F4) may be correlative with the Bunbury Basalt (Coleman et al., 1982). Continental rocks dredged from the southern flank of the Naturaliste Plateau suggest that the feature is cored by continental crust (Beslier et al., 2001), so the volume of volcanic rock potentially related to Bunbury volcanism is unknown. Apparently, neither the area nor the volume of the Bunbury Basalt are of flood basalt province dimensions, which are typically 10^5–10^6 km^2 and 10^6 km^3, respectively. Also, volcanic rocks are not abundant in the continental margin of the Perth Basin (Symonds et al., 1998). So if indeed the Bunbury Basalt ± Naturaliste Plateau volcanic rocks represent the initial output of the Kerguelen hotspot, the underlying anomalous mantle was not significantly hot, wet, or voluminous enough to produce either a continental flood basalt province or a strongly volcanic passive margin despite the enhancing effects of thin, weakened lithosphere on decompressional melting. In marked contrast, voluminous magmatism accompanied ~136- to ~158-Ma continental breakup between Greater India and Australia to the north, creating volcanic margins and perhaps the younger Cuvier and Wallaby Plateaus (F1, F4) northward along the margin of western and northwest Australia (Symonds et al., 1998). To date, no hotspot source or sources have been identified for that voluminous magmatism.

The next phase of magmatism attributed to the Kerguelen hotspot, 110 to 120 Ma, began at least 12 m.y., and perhaps as many as ~45 m.y., after seafloor spreading started between India and Antarctica (Fig. F4). During this phase, the Kerguelen hotspot produced its only features of flood basalt scale on both thinned continental crust (Rajmahal Traps) (Kent et al., 1997) and in an ocean basin (SKP) (Figs. F1, F4). Between ~120 and ~110 Ma, the SKP grew at a high rate (Figs. F3, F4). Magma output rates were also high from ~105 to 100 Ma and ~100 to 95 Ma with the formation of the CKP and Broken Ridge, respectively.

The peak output rates of the Kerguelen hotspot from ~120 to ~95 Ma (Figs. F3, F4) lag initial breakup between India and Antarctica by 12–70 m.y. Corroborating evidence is that no physiographic feature analogous to the Greenland-Scotland Ridge, Chagos-Laccadive Ridge, Walvis Ridge, and Sao Paulo/Rio Grande Plateaus connects Antarctica and the SKP across the Princess Elizabeth Trough and that the East Antarctic continental margin south of the Kerguelen Plateau does not exhibit seismic characteristics that would classify it as strongly volcanic (Stagg, 1985; P.A. Symonds, pers. comm., 2001). Neither does the conjugate continental margin of East India (e.g., Gopala Rao et al., 1997; Chand et al., 2001), although thick sediments of the Bengal Fan mask the margin's basement structure due south of the Rajmahal Traps (e.g., Kent et al., 1997; Subrahmanyam et al., 1999). Thus, unlike the Iceland hotspot and the associated North Atlantic volcanic province and the Tristan hotspot and the associated Paraná/Etendeka flood basalt province, the peak output of the Kerguelen hotspot cannot be correlated temporally or spatially with a major phase of continental breakup and volcanic margin formation. Rather, like the relationship between the Réunion hotspot, the Deccan flood basalt, and the breakup between the Seychelles and West India, (e.g., Müller et al., 2001), the peak output of the Kerguelen hotspot appears to coincide with one or more episodes of microcontinent formation as pieces of East India, such as Elan Bank, broke off and became isolated within oceanic lithosphere. This hypothesis predicts that the portion of the East India continental margin from which Elan Bank and portions of the SKP broke up and separated are to some extent volcanic, despite the observed lack of significant volcanism (e.g., Gopala Rao et al., 1997; Chand et al., 2001). For the Bengal Fan portion of the East Indian margin, however, evaluating this prediction awaits acquisition of high-quality, deep seismic data.

The areal extent of magmatism attributed to the Kerguelen hotspot was very large from ~120 to ~110 Ma. For example, at ~119 Ma, the distance between the Rajmahal Traps and the Bunbury Basalt was ~2000 km, and a similar distance separated the Rajmahal Traps and the Antarctic lamprophyres at ~110 Ma (Figs. F1, F4). The recent $^{40}Ar/^{39}Ar$ age determinations described previously indicate simultaneous volcanism in India (Rajmahal Traps and lamprophyres), Antarctica (lamprophyres), and the Enderby Basin (SKP). That volcanism occurs over such a broad region is not surprising; what is surprising is that magmatic products from a single plume, whether axisymmetric or not, would apparently bypass the relatively young oceanic lithosphere of the Enderby Basin south of the SKP, including active spreading centers and the continent–ocean transition lithosphere of East Antarctica and much of eastern India, to erupt on old continental lithosphere, albeit probably rifted and thinned, of India and Antarctica (Fig. F4).

From ~82 (possibly ~95) to ~38 Ma, the Kerguelen hotspot produced the ~5000-km-long Ninetyeast Ridge. Geochemical evidence suggests that much of it formed relatively close to or at a spreading ridge axis (Frey et al., 1977, 1991; Saunders et al., 1991; Weis et al., 1991; Frey and Weis, 1995), but the lack of any conjugate feature on the Antarctic plate (cf. the Iceland hotspot and the Greenland-Faeroe-Shetland Ridge) casts considerable doubt that the Kerguelen hotspot coincided with a spreading center from ~82 Ma until breakup between the CKP and Broken Ridge at ~40 Ma (Fig. F4). Subsequently, the Antarctic plate moved over the Kerguelen hotspot, and the NKP was constructed on relatively old oceanic lithosphere. From ~30 Ma to the present, magmatic output related to the Kerguelen hotspot has been variable and spatially widespread. The flood basalt of the Kerguelen archipelago formed from ~30 to ~24 Ma (Nicolaysen et al., 2000), and less voluminous alkalic volcanism continued in the archipelago until <1 Ma (Weis and Giret, 1994; Weis et al., 1993, 1998). Since at least 21 Ma, Kerguelen hotspot magmatism has also constructed volcanic edifices on the Cretaceous CKP, including Heard Island (Quilty et al., 1983; Coffin et al., 1986; Weis et al., 2002). Both Heard and McDonald Islands have had historical eruptions (Quilty and Wheller, 2000).

PETROGENESIS OF BASEMENT IGNEOUS ROCKS

Basement sections recovered from 11 drill sites on the Kerguelen Plateau and Broken Ridge (i.e., Leg 119, Site 738; Leg 120, Sites 747, 749, and 750; and Leg 183, Sites 1136, 1137, 1138, 1139, 1140, 1141, and 1142) (Fig. F1) are dominantly tholeiitic basalt (8 of 11 sites) with moderate MgO contents (5–8 wt%) (Figs. F5, F6). Their incompatible element abundance and radiogenic isotopic ratios (Sr, Nd, and Pb) dis-

F5. Total alkalis vs. SiO_2 classification plot, p. 41.

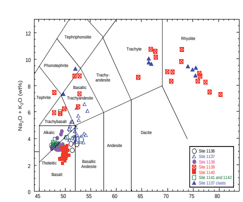

F6. Abundance of TiO_2 vs. MgO, p. 42.

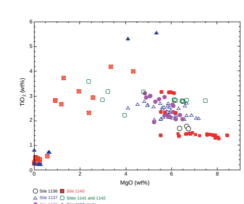

tinguish these LIP lavas from mid-ocean-ridge basalt (Figs. F7, F8, F9). However, at each drill site on the LIP the geochemical characteristics of the basalt require very significant differences in petrogenesis. These differences result largely from (1) changing proportions in source components, namely plume, depleted asthenosphere, and continental lithosphere; (2) geochemical heterogeneity in the source components, especially the plume and continental lithosphere; (3) variable extents of melting; and (4) variable extents and types of postmelting magmatic processes. Following, in order of decreasing eruption age, we discuss the petrogenesis of lavas from each site.

Site 1136: Southern Kerguelen Plateau

Prior to Leg 183, igneous basement of the SKP had been recovered by dredging (Leclaire et al., 1987) and drilling during Legs 119 and 120 (Fig. F1). Basalt from Site 738, the southernmost sampling location, has a tholeiitic composition, but its trace element characteristics and isotopic ratios (Sr, Nd, and Pb) (Figs. F7, F8, F9, F10) clearly reflect a component derived from continental lithosphere, probably crust (Alibert, 1991; Mahoney et al., 1995). Continental crust, especially upper crust, is distinguished by relatively high $^{87}Sr/^{86}Sr$, low $^{143}Nd/^{144}Nd$, high $^{207}Pb/^{204}Pb$ and $^{208}Pb/^{204}Pb$ at a given $^{206}Pb/^{204}Pb$, and relative depletions in abundances of Nb and Ta. In particular, Mahoney et al. (1995) used plots of Δ7/4 and Δ8/4 vs. La/Ta (or equivalently, La/Nb) to show convincingly that SKP basalt from Site 738 contains a significant proportion of a continental component (Fig. F10). Although recycled continental lithosphere could be intrinsic to a mantle plume, the extreme geochemical characteristics of Site 738 basalt (Figs. F7A, F8, F9, F10) are compatible with an alternative hypothesis; that is plume-derived magma assimilated continental lithosphere, probably crust, that was dispersed as fragments into the Indian Ocean asthenosphere or lithosphere as a result of Gondwana breakup (Mahoney et al., 1995; Frey et al., 2000a; see fig. 14c of Frey et al., 2002b). A continental component is not obvious in basalt from the more northerly Sites 749 and 750 on the SKP (Figs. F7C, F8, F9, F10), but Storey et al. (1989) suggested that the relative depletion in Ta (and Nb) in some dredged basalt from the northern SKP may reflect incorporation of sub-Gondwana continental lithosphere into the asthenosphere beneath the Indian Ocean. Consequently, a specific goal of drilling at Site 1136 in the southeast part of the SKP was to evaluate the areal extent of continental lithosphere components in the uppermost igneous basement of the SKP.

The 33.3 m of basement penetration at Site 1136 (Fig. F2) includes three flow units of tholeiitic basalt that were studied by Neal et al. (2002). $^{39}Ar/^{40}Ar$ isotope analyses for plagioclase from Units 1 and 2 yield the oldest ages (~119 Ma) found on the Kerguelen Plateau (Duncan, 2002). The field defined by $^{87}Sr/^{86}Sr$ and $^{143}Nd/^{144}Nd$ of Units 1 and 2 is slightly offset from the field defined by Cenozoic oceanic island basalt associated with the Kerguelen plume (e.g., the Kerguelen archipelago), and $^{206}Pb/^{204}Pb$ is clearly lower in Site 1136 basalt than flood basalt from the archipelago (Figs. F8, F9); this offset to lower $^{206}Pb/^{204}Pb$ is a characteristic difference between Cretaceous Kerguelen Plateau basalt and the lavas forming the Cenozoic Kerguelen archipelago (Fig. F9).

F7. Incompatible element abundances, p. 43.

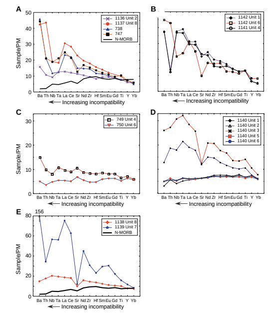

F8. $^{143}Nd/^{144}Nd$ vs. $^{87}Sr/^{86}Sr$ for mafic rocks, p. 45.

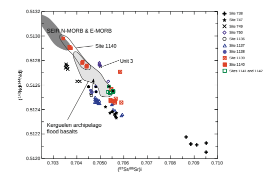

F9. $^{207}Pb/^{204}Pb$ and $^{208}Pb/^{204}Pb$ vs. $^{206}Pb/^{204}Pb$ for mafic rocks, p. 46.

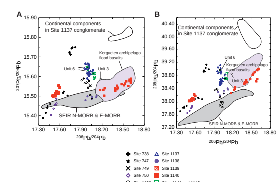

F10. Δ8/4 vs. $(La/Nb)_{PM}$, p. 47.

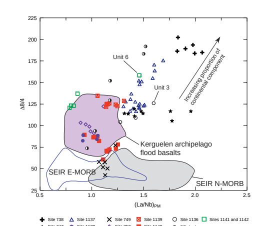

In contrast to basalt from Site 738, the isotopic characteristics and relative abundance of Nb and Ta show that Site 1136 basalt is not highly contaminated with continental crust (Figs. F7A, F8, F9). Based on a Δ8/4 vs. La/Nb plot (Fig. F10), Neal et al. (2002) concluded that basalt from Units 1 and 2 of Site 1136 "have been influenced slightly by continental material." Although the limited recovery, 53 cm, of only highly altered rubbly flowtop hinders detailed interpretation, Unit 3 is isotopically distinct from Units 1 and 2 (e.g., Figs. F8, F9); apparently Unit 3 was derived from a different source than Units 1 and 2 (Neal et al., 2002).

Site 1137: Elan Bank

Site 1137 is on the previously unsampled Elan Bank, a large western salient of the main Kerguelen Plateau that is flanked on three sides by oceanic crust of the Enderby Basin (Fig. F1). The ~152-m basement sequence, composed of seven basaltic flow units and three volcaniclastic sedimentary units (Fig. F2), provided several unanticipated results. Basement Units 1–4, 7, 8, and 10 are ~107- to 108-Ma dominantly tholeiitic to transitional basalt (Fig. F5) with no discernible downhole age progression (Duncan, 2002). However, basement Units 5, 6, and 9 are volcaniclastic sedimentary rocks. Unit 9 is ~17 m of altered crystal-vitric tuff containing ~40% 1- to 2-mm angular crystals of sanidine and quartz. Unit 5 is ~4.4 m of sandstone, dominantly lithic volcanic fragments (75%), but also including feldspar (15%), quartz (5%), and garnet (1%). Unit 6 is ~31 m of conglomerate including clasts ranging from granules to boulders of trachyte, rhyolite, basalt with varied phenocryst assemblages (Fig. F5), and, most surprisingly, rounded cobbles of garnet-biotite gneiss and granitoid. The depositional environment of basement Units 5 and 6 appears fluvial, perhaps associated with a braided river.

Nicolaysen et al. (2001) used U-Pb and Pb-Pb dating techniques to obtain a wide range of ages (534–2457 Ma) for zircon and monazite separated from garnet-biotite clasts in Unit 6 and the overlying sandstone of Unit 5. These dates show that old continental crust dispersed during the breakup of Gondwana resides in the shallow crust of the Kerguelen Plateau. Age constraints (Nicolaysen et al., 2001) and isotopic data for the gneiss clasts (Ingle et al., 2002a) are consistent with a source that originated in the Eastern Ghats of eastern India. Isolation of the Elan Bank microcontinent is inferred to have occurred during a northward ridge jump (i.e., toward India) of the early spreading center in the Enderby Basin (see discussion in "The Kerguelen Hotspot and Indian Ocean Plate Reconstructions," p. 5).

Garnet grains within the gneiss clasts are Fe rich (77–85 mol% almandine) (Nicolaysen et al., 2001), but garnet grains within the sandstone of Unit 5 span a larger range (77–35 mol% almandine). As a result, Reusch and Yates (this volume) suggest that the source area sampled by these sedimentary units included a range of metamorphic facies and variety of bulk compositions, as expected in a continental region composed of pelitic and granitic materials.

Geochemical studies of the conglomerate matrix and diverse clast types by Ingle et al. (2002a) showed that the felsic volcanic clasts (trachyte and rhyolite) are not genetically related to the intercalated basalt. Based on Sr, Nd, and Pb isotopic data, Ingle et al. (2002a) concluded that the felsic volcanic clasts formed by partial melting of evolved upper continental crust.

Prior to drilling at Site 1137, Mahoney et al. (1995) inferred that the continental component in basalt from Site 738 was introduced into plume-derived magmas at shallow depths rather than deeply recycled crust intrinsic to the Kerguelen plume. This inference is supported by the presence of continental crust clasts in the conglomerate at Site 1137. Moreover, at Site 1137 the uppermost basaltic units are largely plume derived, but the plume-derived lowermost basaltic units apparently assimilated continental lithosphere (Figs. F7A, F10) (Weis et al., 2001; Ingle et al., 2002b) What is the proportion of continental component in these contaminated lavas? Ingle et al. (2002b) calculated that the isotopic trends of Site 1137 basalt can be explained by 5% to 7% assimilation of material similar to the garnet biotite gneiss. In detail, these clasts do not have Pb isotopic ratios that are suitable for explaining the trend in Pb isotopic ratios defined by Site 1137 basalt (Fig. F9). Also, the Pb isotopic data show that the crustal components contributing to Site 738 and 1137 basalt are geochemically different and that both differ in Pb isotopic ratios from the clasts of garnet biotite gneiss (Fig. F9) (Weis et al., 2001). Given the heterogeneity of continental crust, this result is not surprising. Ingle et al. (2002b), however, emphasized the striking similarities in Pb isotopic trends between basalt erupted at Site 1137 and the continental flood basalt forming the Rajmahal Traps in northeast India and Bunbury Basalt in Southwest Australia. Although these locations are now widely disparate (Fig. F1), they were closer (~1000 km apart) at their time of formation (Fig. F4), and Ingle et al. (2002b) argued that in each case magmas derived from the Kerguelen plume interacted with Gondwana crust having similar Pb isotopic characteristics.

Site 1138: Central Kerguelen Plateau

A major objective at this drill site was to determine the basement age of the CKP; no reliable age information is available for basalt from Site 747, the only previous drill site on the CKP (Figs. F1, F2). At Site 1138, 22 units of igneous basement were recognized in the 144 m of recovered rock. Particularly surprising were two units of felsic igneous rock overlying tholeiitic basalt (Fig. F2), that is Unit 1, cobbles of flow-banded dacite, and Unit 2, an ~20-m-thick volcaniclastic section interpreted as subaerial pyroclastic flow deposits. No evidence of compositionally evolved, explosively erupted volcanic deposits, such as those at Sites 1137 and 1138, was found during previous drilling on the Kerguelen Plateau. Although the dacite at Site 1138 (Unit 1) may have largely formed by extensive fractional crystallization of magmas similar to the underlying basalt, differences in Sr and Pb (but not Nd) isotopic ratios suggest the possible influence of continental material (Neal et al., 2002). Processes involved in creating these SiO_2-rich igneous units in uppermost igneous basement range from partial melting of continental crust fragments within the oceanic lithosphere (e.g., at Site 1137 the felsic clasts in Unit 6 and the sanidine-rich felsic tuff of Unit 9) (Weis et al., 2001; Ingle et al., 2002a) to combined fractional crystallization and assimilation of continental crust fragments (Unit 1 of Site 1138) (Neal et al., 2002).

Underlying the nonbasaltic rocks at Site 1138 are 20 units of ~5-m-thick tholeiitic to transitional basalt (Fig. F5), some with oxidized flow tops, which are interpreted as subaerial eruptives. $^{40}Ar/^{39}Ar$ data for plagioclase and whole-rock basalt from two flow units indicate an age of 100–101 Ma (Duncan, 2002). These basaltic units have $^{87}Sr/^{86}Sr$,

$^{143}Nd/^{144}Nd$, and $^{206}Pb/^{204}Pb$ ratios that overlap those of lavas from Units 1 and 2 at Site 1136 on the SKP (Figs. F8, F9), suggesting that basalt sources were similar over a large area and over an ~20-m.y. time span. In contrast with basalts from Sites 738, 1136, and 1137, the Site 1138 lavas are not relatively depleted in Nb (Figs. F7E, F10). Consequently, Neal et al. (2002) concluded that there is no significant influence of continental crust in Site 1138 basalt.

The basalt units at Site 1138 increase in Mg/Fe from the lowermost to uppermost unit (i.e., Mg/Fe increases with decreasing eruption age) (Shipboard Scientific Party, 2000; Neal et al., 2002). With decreasing Mg/Fe, the abundance of incompatible elements increases (e.g., TiO_2) (Fig. F6) and the abundance of compatible elements decreases. Neal et al. (2002) used major and trace element abundances in these basaltic units to show that the data are inconsistent with closed-system fractional crystallization. They concluded that the compositional variations of Site 1138 lavas can be explained by an open-system process involving periodic replenishment of a fractionating basaltic magma with plagioclase and clinopyroxene as major fractionating phases; for example, the relative depletion in Sr (Fig. F7E) reflects plagioclase fractionation. Clearly, during the final growth stage of the CKP, the magma flux from the mantle was sufficiently low to enable extensive fractional crystallization of basaltic magma and eventually the formation of dacitic magma by combined fractional crystallization and assimilation.

Sites 1141 and 1142: Broken Ridge

Broken Ridge and the CKP formed as a single entity during Cretaceous time, but they were separated at ~40 Ma by the newly formed SEIR (e.g., McKenzie and Sclater, 1971; Houtz et al., 1977; Mutter and Cande, 1983). The igneous basement of central and eastern Broken Ridge has been sampled at three locations by dredging (Fig. F1). The dredged rocks are tholeiitic basalt that yielded ages from ~61 to 89 Ma (Duncan, 1991); these ages are no longer considered reliable (Duncan, pers. comm., 2002). They are quite variable in their geochemical characteristics, but basalt from eastern Broken Ridge (Dr 8) contains a continental component (Fig. F10) (Mahoney et al., 1995).

At Sites 1141 and 1142 our goal was to obtain in situ basement in order to document more fully the age of Broken Ridge and to document further the areal extent of basalt with isotopic and trace element characteristics that indicate the presence of a continental component. During operations at Site 1141 the drill string became stuck, and the hole was abandoned after only ~72 m of basement penetration, which included six basement units (Fig. F2). At Site 1142, only ~800 m away from Site 1141, ~51 m of basement penetration recovered six basement units (Fig. F2).

$^{39}Ar/^{40}Ar$ isotope data of whole-rock samples from Sites 1141 and 1142 yield ages of 94–95 Ma (Duncan, 2002), significantly older than the ages inferred for the dredged basalt. In contrast to the dredges on Broken Ridge, which recovered only tholeiitic basalt (Mahoney et al., 1995), all of the Site 1141 and 1142, basement units are slightly alkalic, except for the lowermost Unit 6 at Site 1142, which is tholeiitic basaltic andesite (Fig. F5). This alkalic-tholeiitic classification was initially made using a total alkalis-SiO_2 plot, and it is confirmed by the generally lower abundance of incompatible elements in the tholeiitic basaltic andesite

(Neal et al., 2002). An important result is that only Unit 6 is relatively depleted in Nb and Ta (Fig. F7B).

Also in contrast with the dredged tholeiitic basalt from Broken Ridge, basalts from Sites 1141 and 1142 span only a small range in $^{87}Sr/^{86}Sr$ and $^{143}Nd/^{144}Nd$, which is at the enriched end (i.e., high $^{87}Sr/^{86}Sr$ and low $^{143}Nd/^{144}Nd$) of the field for Kerguelen archipelago flood basalt (Fig. F8). These ratios overlap with the field proposed for the Cenozoic Kerguelen plume and may represent the major component in the plume tail (Neal et al., 2002). Relative to the alkalic basalt units at Site 1141 and 1142, the tholeiitic basalt of Unit 6 at Site 1142 has the lowest $^{206}Pb/^{204}Pb$ and highest $^{207}Pb/^{204}Pb$ and $^{208}Pb/^{204}Pb$ (Fig. F9). In Pb-Pb isotopic plots, Unit 6 lavas are within the field for the lowermost basaltic units at Site 1137 (Fig. F9).

At $^{206}Pb/^{204}Pb$ of ~18, basalt from several sites define a near-vertical trend in plots of $^{207}Pb/^{204}Pb$ and $^{208}Pb/^{204}Pb$ vs. $^{206}Pb/^{204}Pb$ (Fig. F9) (i.e., $^{208}Pb/^{204}Pb$ increases from Site 749 to Site 1138 to Site 1136 to Sites 1141/42 and Site 1137) (Fig. F9). This increase in $^{208}Pb/^{204}Pb$, as measured by $\Delta 8/4$, is correlated with a relative deficiency in Nb, as measured by $(La/Nb)_{PM}$ (Fig. F10); relatively high $\Delta 8/4$ and $(La/Nb)_{PM}$ indicate an increasing role for a continental component (Mahoney et al., 1995; Ingle et al., 2002b; Neal et al., 2002). Among the Site 1141 and 1142 basement units, only Unit 6 from Site 1142 is characterized by high $\Delta 8/4$ and $(La/Nb)_{PM} > 1$ (Fig. F10). This unit, like Dr 8 samples from eastern Broken Ridge ~100 km to the east, may contain a continental component (Neal et al., 2002). In summary, the geochemical variability of Broken Ridge basaltic basement documented by basalt from three dredge sites and two drill sites shows that the uppermost basement at Broken Ridge is highly heterogeneous, much like the igneous basement of the CKP and SKP.

Site 1139: Skiff Bank

Skiff Bank is a bathymetric and gravimetric high on the NKP, ~350 km west-southwest of the Kerguelen archipelago, that is bathymetrically continuous with the NKP (Fig. F1). Prior to Leg 183, Skiff Bank was interpreted to be related to the NKP. Also prior to Leg 183, the submarine basement of the NKP was believed to be of Cenozoic age (<40 Ma) and Skiff Bank had been proposed to be the present-day location of the Kerguelen plume (e.g., Duncan and Storey, 1992; Müller et al., 1993). During a predrilling survey cruise for locating Site 1139, Skiff Bank was dredged and a wide range of rock types coated with Fe-Mn crust were recovered (Weis et al., 2002). These rocks have not been studied, but they provide no evidence for recent volcanism.

As at Site 1137 on Elan Bank, the basement recovery at Site 1139 had many surprises. Basement penetration reached ~232 m, and 19 igneous units were identified (Fig. F2). All of the igneous units have <4.5 wt% MgO (Fig. F6). Despite complications arising from intense postmagmatic alteration there is no doubt that the magmas were alkalic in composition (Fig. F5) (Kieffer et al., 2002); for example, excluding elements controlled by fractionating phases, such as Sr by plagioclase, Site 1139 lavas have higher abundances of incompatible elements than all other mafic lavas recovered during Leg 183 (Fig. F7). The basement sequence is bimodal, with a 73-m-thick series of trachybasaltic lava flows sandwiched between felsic (trachyte and rhyolite) volcanic rocks (Figs. F2, F5) (Kieffer et al., 2002). No tholeiitic basalt, the dominant basalt type at all other Kerguelen Plateau drill sites, is present at Site 1139 (Fig. F5). Ar-Ar geochronology of whole-rock samples and feldspar separates from these felsic rocks yield ages of ~68–69 Ma (Duncan, 2002). Clearly, Skiff Bank is not a site of recent volcanism and this part of the NKP is not Cenozoic in age. Furthermore, the magmatism at Skiff Bank was alkalic in composition, like basalt erupted on Cenozoic islands constructed on the plateau, but unlike sampled regions of the CKP and SKP.

Kieffer et al. (2002) inferred that the subaerially erupted lava units at Site 1139 represent part of a shield volcano built on a volcanic plateau of unknown age; shield volcanoes constructed on the Ethiopian plateau may be an analogy. The felsic and mafic lavas at Site 1139 have similar Nd and Pb isotopic ratios (Sr is perturbed by alteration), and Kieffer et al. (2002) infer that felsic lavas formed as partial melts of mafic rocks. In contrast to the intermediate $^{206}Pb/^{204}Pb$ (~18) and near-vertical $^{207}Pb/^{204}Pb$ and $^{208}Pb/^{204}Pb$ vs. $^{206}Pb/^{204}Pb$ trends defined by basalt from Sites 749, 1136, 1137, 1138, 1141, and 1142, the mafic lavas at Site 1139 have low $^{206}Pb/^{204}Pb$, ~17.5, much like basalt from Sites 747 (CKP) and 750 (SKP) (Fig. F9). Site 747 basalt is also depleted in Nb (Fig. F10); therefore, Frey et al. (2002b) inferred that such low $^{206}Pb/^{204}Pb$ ratios reflect a component derived from lower continental crust. However, like basalt from Site 750, the mafic lavas from Site 1139 are not highly depleted in Nb (Figs. F7E, F10).

Site 1140: Northern Kerguelen Plateau

Site 1140 is on the northernmost part of the NKP, 270 km north of the Kerguelen archipelago (Fig. F1). The boundary between the NKP and Australia-Antarctic Basin is only 5 km north of Site 1140. Major objectives at this site were to test the hypothesis that the uppermost igneous basement of the NKP formed at <40 Ma and to compare the igneous basement with the <30-Ma flood basalt forming the Kerguelen archipelago.

Drilling at Site 1140 penetrated 88 m of basement rocks, which included five units of tholeiitic pillow basalt (Fig. F5) and an interbedded 1-m-thick carbonate unit (Fig. F2). These are the only sampled basement lavas in the LIP that erupted in a submarine environment. Earliest Oligocene (32.8–34.3 Ma) nannofossil and foraminifer oozes overlie Unit 1 (Persico and Wise, this volume). A magnetic reversal between Units 1 and 2 is inferred to be C13n/C13r (33.6 Ma). These age constraints are consistent with ages of ~34 Ma determined by Ar-Ar geochronology on plagioclase and whole rocks (Duncan, 2002).

At 34 Ma the location of Site 1140 was within 50 km of the SEIR (Weis and Frey, 2002). Each of the five pillow basalt units is geochemically distinct, but they broadly divide into two groups, (1) Units 2 and 3, which are relatively enriched in P_2O_5 and TiO_2 and highly incompatible elements, and (2) Units 1, 5, and 6, which have incompatible element abundances similar to mid-ocean-ridge basalt (MORB) (Figs. F6, F7D). The latter group has lower $^{87}Sr/^{86}Sr$, higher $^{143}Nd/^{144}Nd$, and lower Pb isotopic ratios (Figs. F8, F9). The isotopic differences between each unit can be explained by mixing between plume-derived magmas (represented by lavas erupted in the Kerguelen archipelago) and SEIR MORB. Consistent with the proximity of this site to the SEIR at the time of eruption (34 Ma), the SEIR MORB component is dominant (60%–99%); the isotopic ratios (Sr, Nd, and Pb) of the youngest lavas (Unit 1) overlap with SEIR MORB (Figs. F8, F9) (Weis and Frey, 2002). In contrast to all other igneous basement recovered from the Kerguelen Plateau, which has $^{206}Pb/^{204}Pb$ < 18.2, the Site 1140 lavas range to higher $^{206}Pb/^{204}Pb$; those with the largest proportion of plume component have Pb isotopic ratios overlapping with basalt forming the Kerguelen archipelago (Fig. F9).

Four of the Site 1140 pillow basalt units have sufficient glass for geochemical studies. Ion microprobe analyses of these glasses by Wallace (2002) also showed that the compositions of these basaltic units can be explained by mixing of MORB and plume-derived magmas. Importantly, these glasses provide information not available from whole-rock studies. In particular, Wallace (2002) found that units with MORB-like Sr, Nd, and Pb isotopic ratios have volatile (H_2O, S, and Cl) contents similar to MORB, but the two units with a higher proportion of a plume-derived component have higher water contents (0.44–0.69 wt%). Despite their higher contents of H_2O, these units have H_2O/Ce ratios less than those of MORB. Apparently, the Kerguelen plume was not a wet spot (Schilling et al., 1980; Bonatti, 1990), requiring that melting in the plume was caused by relatively high mantle temperature and not due to anomalously high mantle H_2O contents.

MANTLE SOURCES, PLUME-LITHOSPHERE INTERACTIONS, AND PLUME MODELS

The interplay between Kerguelen hotspot magmatism and Indian Ocean plate motions since the Early Cretaceous has produced a complicated record to decipher (Fig. F4). What is clear, however, from the preceding discussion, as well as from a large body of published work, is that the Kerguelen hotspot challenges many widely held assumptions about mantle plumes (Wilson, 1963, 1965; Morgan, 1971, 1972).

Current plume models predict massive magmatism coeval with continental breakup (e.g., White and McKenzie, 1989; Anderson, 1995), voluminous magmatism associated with an individual plume exploiting thin and weak lithosphere (e.g., Artyushkov et al., 1980; White and McKenzie, 1989, 1995; Thompson and Gibson, 1991; Sleep, 1996, 1997), and temporal scales of <5 m.y. for plume-head–type magmatism (e.g., Campbell and Griffiths, 1990). In contrast, peak output rates for magmatism attributed to the Kerguelen plume lasted for 25 m.y. Apparently, massive magmatism did not accompany the breakup of India and Antarctica but did accompany the breakup between India and Elan Bank. Extensive Early Cretaceous magmatic activity did not affect large areas of relatively young oceanic and transitional lithosphere, including spreading center segments between the SKP and Antarctica and along much of the margin of East India, yet produced lamprophyres by partial melting of the relatively old continental lithosphere of eastern India and East Antarctica.

Magmas associated with individual plumes typically show significant geochemical heterogeneity (e.g., in radiogenic isotopic ratios). Such heterogeneity is interpreted to represent intrinsic heterogeneities within the plume and mixing of plume material with entrained asthenosphere and overlying lithosphere. A depleted component in basalt associated with plumes is interpreted to reflect components derived from MORB-related asthenosphere and lithosphere (e.g., Galapagos; Harpp and White, 2001) or a depleted component intrinsic to the plume (e.g., Iceland; Kempton et al., 2000). For Site 1140 in the

NKP, Weis and Frey (2002) favor mixing of melts derived from the Kerguelen plume and nearby (<50 km) SEIR. For lavas erupted in the Kerguelen archipelago, more distant from the SEIR at the time of eruption, the origin of the depleted component is under debate (Doucet et al., 2002; Frey et al., 2002a).

However, what distinguishes lavas associated with the Kerguelen plume is the diversity of radiogenic isotopic ratios ranging from values typical of MORB to those of continental crust (Figs. F8, F9). This range exceeds that of lavas associated with all other oceanic hotspots. Although erupted in an oceanic setting, some Kerguelen Plateau and Broken Ridge rocks contain abundant evidence for a continental lithosphere component. In particular, basalt from Site 738 in the SKP (Fig. F1) with $^{87}Sr/^{86}Sr$ = ~0.709 (Fig. F8) is interpreted "to have inherited its isotopic signature from old lithospheric mantle underlying the East Antarctica and southwestern Australia continental margins, rather than from the Kerguelen hotspot" (Alibert, 1991), and Mahoney et al. (1995) suggest that at Site 738 continental lithosphere was incorporated into the plume at "relatively shallow levels." Relative to Site 738 basalt, lavas from Site 1137 are not as extreme in Sr and Nd isotopic ratios (Fig. F8) but their Pb isotopic ratios (Fig. F9) also suggest a role for continental lithosphere (Ingle et al., 2002b). In this case, the clasts of ancient continental crust in a conglomerate intercalated with Site 1137 basaltic lava flows confirm the shallow origin of the continental component. Within the Cretaceous parts of the Kerguelen Plateau and Broken Ridge, continental components are widespread, ranging from Site 738 in the SKP to Site 747 in the CKP to Site 1137 on Elan Bank to Site 1142 on Broken Ridge. However, a continental component is not pervasive. Alkalic basalt from Broken Ridge (95 Ma) and tholeiitic basalt from Site 1136 (119 Ma in SKP) and Site 1138 (100 Ma in CKP) have Sr and Nd isotopic ratios (after correction for age differences) similar to Cenozoic lavas erupted in the Kerguelen archipelago (Fig. F8). Also, the role of a continental component in lavas associated with the Kerguelen hotspot has diminished from the Cretaceous to present; that is, a continental component is not evident in lavas forming the Ninetyeast Ridge (Frey and Weis, 1995) and the Kerguelen archipelago (e.g., Frey et al., 2002a; Weis et al., 2002), and only a single trachyte from Heard Island has a continental isotopic signature (Barling et al., 1994).

At three drill sites (747, 750, and 1139) on the Kerguelen Plateau, Pb isotopic data require a component with unusually low $^{206}Pb/^{204}Pb$ ratios (Fig. F9). The origin of this component, which is similar to the EM-1 oceanic island component, is not well constrained; Frey et al. (2002b) argue for a lower continental crust origin (Sites 747 and 750), but Kieffer et al. (2002) conclude that the "volcanic rocks of Site 1139 show no convincing evidence of continental material."

In summary, the Kerguelen hotspot shows longer-lived voluminous magmatism and more complex plume-lithosphere interactions than predicted by current plume models. As alternatives to incubating single plume head models (e.g., Kent et al., 1992; Saunders et al., 1992; Storey et al., 1992), we suggest two possibilities: (1) that the magmatism attributed to the Kerguelen plume did not arise from a single plume source, but to multiple plume sources (e.g., Burke, 2001; Wilson and Patterson, 2001); or (2) that a single plume source accounts for the magmatic products attributed to the Kerguelen plume, but that vigorous mantle circulation during Early Cretaceous time (e.g., Larson, 1991; Stein and Hofmann, 1994; Eldholm and Coffin, 2000) caused strong mantle shear flow that split the initial Kerguelen plume conduit into several "diapirs" of varying sizes, buoyancies, and mantle ascent rates (e.g., Olson, 1990; Steinberger and O'Connell, 1998).

Multiple sources for regional hotspot volcanism are suggested by tomographic images of the lowermost mantle that show heterogeneous slow regions in which slower, D″ hotspots are embedded (e.g., Garnero, 2000). Multiple fingerlike convective instabilities in the upper mantle have recently been proposed to explain the Tertiary–Quaternary volcanism of western and central Europe (Wilson and Patterson, 2001). If multiple mantle plumes can arise from individual heterogeneous slow regions at either the core mantle boundary or the 670-km discontinuity (i.e., the first alternative), then much, if not all, of the temporal and spatial variability displayed by the volcanic products attributed to the Kerguelen hotspot could be explained. This scenario might also explain some but not all of the geochemical heterogeneity in magma sources inferred from the variable radiogenic isotope ratios in basalt associated with the Kerguelen hotspot (e.g., Figs. **F7, F8**). If a plume is geochemically heterogeneous, as seems likely, the second alternative, splitting of a single plume into several diapirs, can also explain temporal, spatial, and geochemical variability in the volcanism. In Early Cretaceous time, separate mantle diapirs could have produced the Bunbury Basalt, the SKP, the Rajmahal Traps/Indian lamprophyres, the Antarctic lamprophyres, and the CKP/Broken Ridge. Additionally, separate mantle diapirs from the same source region could account for massive Cretaceous volcanism offshore Western Australia that has not so far been linked to the Kerguelen hotspot (e.g., Symonds et al., 1998). As mantle circulation rates slowed during the Late Cretaceous, a single plume conduit could have become continuous and long-lived, producing the Ninetyeast Ridge. Thereafter, old oceanic lithosphere, slow Antarctic plate motion relative to the plume conduit, and thickened Cretaceous Kerguelen Plateau lithosphere may account for the lack of a well-defined hotspot trace since 40 Ma.

Little is known about how the mass and energy fluxes of mantle plumes varies with time. Hawaii, the prototypical plume with its continuity of magma output over time (e.g., Duncan and Clague, 1985), is probably an end-member of the spectrum. At the other end of the spectrum are short-lived, massive bursts of flood basalt volcanism that lack any obvious subsequent volcanic record (e.g., the Central Atlantic magmatic province) (Marzoli et al., 1999). The Kerguelen plume appears to lie somewhere in the middle of this spectrum, as well-defined hotspot tracks are difficult to discern both before and after the creation of Ninetyeast Ridge. Finally, the obvious role for a continental component at several locations in the Kerguelen Plateau and Broken Ridge shows that even in an oceanic setting a plume can interact with continental lithosphere.

ERUPTION ENVIRONMENT AND IMPACT

Subsidence of the Kerguelen Plateau

The subsidence of oceanic plateaus is believed to result from cooling and contraction of the lithospheric plate on which the plateau is constructed (Detrick et al., 1977). Evidence from ODP Legs 119, 120, and 183 clearly demonstrates that large parts of the SKP and CKP that are now submarine were originally subaerial during plateau construction (Coffin, Frey, Wallace, et al., 2000; **Mohr et al.,** this volume). If the SKP had subsided at similar rates as normal oceanic lithosphere, then original maximum elevations would have been on the order of 1 to 2 km above sea level and much of the SKP's ~500,000-km^2 area would at one time have been above sea level (Coffin, 1992).

A major source of uncertainty in assessing oceanic plateau subsidence is estimating original depth (e.g., from microfossils) or elevation above sea level at the time of eruption. Wallace (2002) used dissolved volatiles, whose concentrations are pressure dependent, in pillow rim glasses at Site 1140 on the NKP to estimate original eruption depths. The results suggest an eruption depth of 870 ± 80 m. After taking account of the effect of sediment loading on subsidence (Crough, 1983), this leads to an estimated subsidence for the NKP of 1664 m since 34 Ma (Fig. **F11**). This value is in excellent agreement with the prediction for 34-Ma normal Indian Ocean lithosphere (Detrick et al., 1977). Although subsidence estimates for the CKP and SKP are more uncertain, Wallace (2002) used ages of the oldest marine sediments at existing drill sites to show that most locations subsided by amounts that are consistent with expectations for normal oceanic lithosphere (Fig. **F11**). This suggests either that the thermal regime typically associated with cooling oceanic lithosphere, despite some embedded continental components, is mainly responsible for the plateau's subsidence behavior, or that the thermal anomaly associated with the Kerguelen plume reset the thermal age of the continental lithosphere embedded in the plateau to near zero. The one site (Site 1139) that appears to have anomalous subsidence (Fig. **F11**) is located on Skiff Bank, a bathymetric and gravimetric high ~350 km west-southwest of the Kerguelen archipelago (Fig. **F1**). Volcanic rocks recovered from Site 1139 have been dated at 68–69 Ma (Duncan, 2002), but Skiff Bank appears to be structurally related to the NKP, on which flood basalt eruptions occurred until ~24 Ma (Frey et al., 2000b). **Reusch** (this volume) uses data for benthic foraminifers to show that Skiff Bank has been at a depth of 1000–2000 m from the early Oligocene to the present. He suggests that Skiff Bank subsided ≥1–2 km during the first 35 m.y. following emplacement of the volcanic rocks (so that originally subaerial rocks reached a water depth of 1–2 km), but that subsequently their subsidence was minimal. An alternative is that because Skiff Bank is structurally related to the NKP, thermal subsidence of Skiff Bank might have been minimal for several tens of millions of years after its formation, due to dynamic uplift associated with the Kerguelen hotspot, thermal rejuvenation of the lithosphere, or a combination thereof. This model is compatible with the data for benthic foraminifers if Skiff Bank began to subside like normal oceanic lithosphere starting at ~45 Ma (i.e., ~25 m.y. following emplacement).

F11. Subsidence estimates for the Kerguelen Plateau vs. eruption age of basement basalts, p. 48.

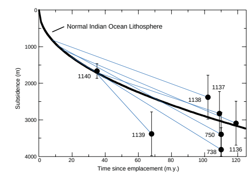

Volatile Release to the Environment during Formation of the Kerguelen Plateau

The release of volatiles such as CO_2, S, Cl, and F accompanying eruption of enormous volumes of basaltic magma during formation of the Kerguelen Plateau and Broken Ridge probably had significant environmental consequences. The role of subaerial volcanic eruptions (Barron, Larsen, et al., 1989; Schlich, Wise, et al., 1989; Coffin, 1992; Coffin, Frey, Wallace, et al., 2000) is significant in this regard because basaltic magmas are nearly completely degassed during subaerial eruptions, whereas hydrostatic pressure inhibits vesiculation and degassing of relatively soluble volatile components (H_2O, S, Cl, and F) during deepwater submarine eruptions (Moore, 1970; Moore and Fabbi, 1971; Unni and Schilling, 1978). In contrast to the more soluble magmatic volatiles, the very low solubility of CO_2 causes it to be mostly degassed even at abyssal depths (Gerlach, 1989).

Determining the volatile fluxes from Kerguelen Plateau magmatism to the environment is difficult because of relatively poor knowledge about primary magmatic volatile contents, magma volume fluxes through time, and the proportion of volcanic activity that was subaerial or in a shallow submarine environment. Nevertheless, it is possible using existing data to make order of magnitude estimates for volatile release in order to consider potential environmental effects. The magma output rate of the Kerguelen hotspot between 120 and 95 Ma, when the SKP, CKP, and Broken Ridge were formed, was ~1 km^3/yr (Coffin et al., 2002) (Fig. **F3**). The magma output rate appears to have decreased after that time (95 to ~25 Ma) to values of ~0.1 km^3/yr. Based on these output rates, the S contents of enriched Site 1140 glasses, and assuming that 50% of the SKP, CKP, and Broken Ridge formed by subaerial eruptions (Coffin, 1992), the estimated S flux to the atmosphere from 120 to 95 Ma would have been 1.4×10^{12} g S/yr (Wallace, 2002). This value is ~13% of the current global flux of S to the atmosphere from subaerial volcanic eruptions (Andres and Kasgnoc, 1998).

An important factor that would have increased the environmental consequences of volcanic S release during formation of the Kerguelen Plateau is the high latitude at which the plateau formed (Frey et al., 2000a). In most basaltic eruptions, released volatiles remain in the troposphere, but at high latitudes, the tropopause is relatively low. As a result, large mass flux basaltic fissure eruption plumes have the potential to transport SO_2 and other volatiles into the stratosphere (Stothers et al., 1986; Self et al., 1998). Sulfuric acid aerosol particles that form in the stratosphere after such eruptions have a longer residence time and greater global dispersal than if the SO_2 remains in the troposphere, thereby resulting in greater effects on climate and atmospheric chemistry. Although the value of 1.4×10^{12} g S/yr estimated above for the period of Kerguelen Plateau formation from 120 to 95 Ma is only ~13% of the current global flux of S from subaerial volcanic eruptions, it is comparable in magnitude to the estimate of ~0.2×10^{12} to 2×10^{12} g S/yr injected into the stratosphere by explosive eruptions (Pyle et al., 1996).

The magma output rates of Coffin et al. (2002) can also be used to estimate the magnitude of volcanic CO_2 release during formation of the SKP, CKP, and Broken Ridge. Assuming a range in primary CO_2 contents based on normal MORB, enriched MORB, and ocean-island basalt magmas (~0.2–0.6 wt% CO_2) leads to a range of estimates from 0.5×10^{13} to 1.4×10^{13} g CO_2/yr released from Kerguelen Plateau volcanism from 120 to 95 Ma. This is ~5% to 10% of the current global annual flux of CO_2 released by mid-ocean-ridge and subduction zone volcanism (Gerlach, 1991; Varekamp et al., 1992). Although the magnitude of CO_2 release from Kerguelen Plateau volcanism appears to be relatively small compared to the total global volcanic flux, a recent reconstruction of atmospheric CO_2 variations during the last 300 m.y. (Retallack, 2001) shows two periods of pronounced CO_2 increase that correspond to the times of formation, respectively, of the SKP and CKP. It should be pointed out, however, that the latter period also partially overlaps with formation of both the Caribbean LIP and the Madagascar flood basalt (Coffin and Eldholm, 1994; Eldholm and Coffin, 2000).

Explosive Felsic Volcanism

Highly explosive felsic eruptions, such as those that produced the pyroclastic deposits on Elan Bank, Skiff Bank, and the CKP, can also inject both particulate material and volatiles (SO_2 and CO_2) directly into the stratosphere (McCormick et al., 1995). The previously unrecognized significant volume of explosive felsic volcanism that occurred when the Kerguelen Plateau and Broken Ridge were subaerial would have further contributed to the effects of this plume volcanism on global climate and environment (Frey et al., 2000a). The total volume of felsic volcanic rocks is poorly constrained, but Leg 183 drilling results indicate that they account for a significant fraction of the volcanic deposits erupted during the final stages of magmatism at several locations on the Kerguelen Plateau.

Analyses of rhyolitic glass inclusions trapped in quartz and sanidine phenocrysts in the tuff at Site 1137 on Elan Bank indicate dissolved magmatic H_2O concentrations of 2 to 6 wt% (Wallace et al., 2000). Such concentrations are sufficient to sustain a powerful Plinian eruption column that can reach stratospheric altitudes (Wilson et al., 1980). Although dissolved S contents of the inclusions are relatively low (P.J. Wallace, unpubl. data), the presence of significant CO_2 makes it likely that the felsic magmas were vapor saturated before eruption. This is important because the vapor phase may contain significant S (e.g., Scaillet et al., 1998). As a result, eruptions of vapor-saturated silicic magmas typically release large amounts of SO_2 derived from the vapor phase, despite the very low concentrations of dissolved S in such magmas (Wallace, 2001).

Environmental Effects of Submarine Hydrothermal Activity

In addition to the potential environmental effects of subaerial volcanism, submarine volcanism and hydrothermal activity during formation of the Kerguelen Plateau and Broken Ridge may also have had important effects on ocean chemistry. Duncan (2002) notes that the seawater Sr isotopic evolution curve exhibits a decline from ~122 to 112 Ma and suggests that this results from large contributions of relatively unradiogenic Sr from hydrothermal activity. Formation of much of the submarine Ontong Java Plateau in the western Pacific at ~122 Ma (Tejada et al., 1996) may also have contributed significantly to seawater Sr changes. However, the importance of hydrothermal activity during formation of oceanic plateaus has not been established. For the Kerguelen Plateau and Broken Ridge a potentially major source of Sr is weathering and erosion of subaerial basalt flows and subsequent riverine transport of Sr to the oceans. Duncan (2002) concludes that if the decrease in seawater radiogenic Sr from 122 to 112 Ma is caused by Kerguelen Plateau hydrothermal activity, then significant submarine volcanism must have ceased between ~115 and ~93 Ma. The latter is the next time period when a sharp decrease in the seawater Sr isotopic evolution curve is seen. Based on new radiometric ages, Duncan (2002) also suggests that rapid submarine construction of the SKP by 118–119 Ma may have contributed to a global environmental crisis recorded by widespread marine black shales (global anoxic event OAE1). Formation of much of the submarine Ontong Java Plateau in the western Pacific at

~122 Ma (Tejada et al., 1996) may also have contributed significantly to this anoxic event.

Subaerial Lava Flow Emplacement Mechanisms and Alteration

A wide variety of mafic subaerial lava types were recovered during Leg 183. A review of the characteristics of these lava types and a refined method for classifying flows recovered in core based on macroscopic textural features is provided by Keszthelyi (this volume). Excluding flow units that cannot be classified because of poor core recovery or intense alteration, Keszthelyi (this volume) concludes that of 30 flow units from Sites 1136, 1137, 1138, and 1139, 7% are slab pahoehoe, 13% are aa, 27% are pahoehoe, and 53% are rubbly pahoehoe. The last of these—rubbly pahoehoe—refers to a lava type that has a flow top composed of broken pieces of smaller pahoehoe lobes. Keszthelyi considers rubbly pahoehoe to be distinct from slab and other recognized types of pahoehoe and suggests that it is a common flow type in Iceland and the Columbia River Basalt Group.

Kurnosov et al. (this volume) show that the subaerial basalts have been variably altered by low-temperature hydrothermal processes (<120°C), and some have been affected by subaerial weathering. Important secondary minerals associated with the hydrothermal alteration include smectites and chlorite minerals. Alteration of the subaerial basalts appears to be related primarily to horizontal fluid flow within permeable contact zones between lava flows (Kurnosov et al., this volume). No soil horizons between basalt flows were recovered at any of the Leg 183 drill sites (Coffin, Frey, Wallace, et al., 2000), but this could be due to the difficulty of recovering thin layers of soft material between basalt during rotary core barrel coring rather than the real absence of soils.

PALEOENVIRONMENTS AND PALEOCEANOGRAPHY

Strategically situated for high-latitude paleoceanographic studies in the southern Indian Ocean, the Kerguelen Plateau contains a record of changing paleoenvironmental and paleoceanographic conditions extending back to Early Cretaceous time. During the Cretaceous period, characterized by relatively warm ocean waters and high eustatic sea level, the Kerguelen Plateau was constructed in a small but expanding Indian Ocean. During Tertiary and Quaternary time, global climate cooled and ice sheets waxed and waned. Today, most of the Kerguelen Plateau lies south of the Antarctic Polar Frontal Zone (Antarctic Convergence) and beneath the main flow of the Antarctic Circumpolar Current. Leg 183's six drill sites on the plateau have yielded important information on Cretaceous paleoenvironments and on the Tertiary development and evolution of these two major physical oceanographic features, which have had and continue to have major effects on global climate and surface water circulation.

Cretaceous

Paleobotanical and palynological data from Site 1138 on the CKP (Figs. F1, F2) provide a detailed picture of the mid-Cretaceous geological and paleovegetational history of the Kerguelen Plateau. Dark, organic-rich silty claystone with many wood fragments and fern remains, certainly of terrestrial origin (Mohr et al., this volume), directly overlies the ~100- to 101-Ma volcanic basement (Duncan, 2002). These terrestrial strata are of late Albian to earliest Cenomanian age, as dated by sporomorphs, and show that parts of the CKP were subaerial at least until late Albian time (Mohr et al., this volume). A diverse high-latitude flora, probably in a dense conifer forest with various fern taxa and early angiosperms in the undergrowth, covered the CKP. Although the vegetational character did not change over this time interval, varying percentages of several sporomorph groups seem to show possibly cyclic abundance variations, perhaps caused by Milankovitch-type events (Mohr et al., this volume). Uppermost Cenomanian to Coniacian sediments are of open marine origin and contain high-diversity dinocyst assemblages.

Late Cretaceous and Danian foraminifers recovered from Site 1138 on the CKP, a fishing vessel's dredge on the CKP, and *Eltanin* core E54-7 in the Labuan Basin (Figs. F1, F2) have yielded paleoceanographic information about that time interval (Quilty, this volume; Holbourn and Kuhnt, 2002). The benthic foraminiferal succession at Site 1138 records the evolution of the CKP from a subaerially exposed platform in Cenomanian time to a bathyal, pelagic environment in early Turonian (Holbourn and Kuhnt, 2002). The pelagic assemblages strongly resemble temperate, open-shelf, bathyal assemblages in the Northern Hemisphere, reflecting prevalent warm, high-latitude temperatures, open oceanic gateways, and a dynamic trans-hemispheric global circulation. The distribution of upper bathyal benthic foraminifers was strongly modulated by carbon flux and fluctuations in oxygenation, although local hydrography and taphonomic processes also played an important role (Holbourn and Kuhnt, 2002). Biofacies changes during late Cenomanian and early Turonian time relate mainly to environmental change and taphonomic bias and do not appear to be linked to true extinction and radiation events (Holbourn and Kuhnt, 2002). Cenomanian–Turonian time was warmer than the subsequent Campanian–Maastrichtian epochs, when the region was in the cool Austral Faunal Province (Quilty, this volume). Late Campanian and Maastrichtian benthic foraminifers are dominated by epifaunal species, suggesting little upwelling and a high degree of oxygenation. Late Maastrichtian foraminifers from the dredge site have a high infaunal content, consistent with significant upwelling and lower oxygenation near the northeast edge of the CKP (Quilty, this volume). The dominant benthic species remains constant through the Upper Cretaceous section at Site 1138.

Planktonic foraminiferal fauna of the Kerguelen Plateau recovered from Sites 1135, 1136, and 1138 have permitted improvement of the biostratigraphic framework for the Southern Ocean region, especially for Turonian–Santonian time (Petrizzo, 2001). Several low- and mid-high–latitude bioevents are useful for correlation across latitudes. Moreover, planktonic foraminiferal assemblages from the Turonian–Coniacian succession throughout the Cretaceous Kerguelen sedimentary sequence clearly indicate affinities with warm-temperate Cretaceous faunas (e.g., Exmouth Plateau), whereas the planktonic fauna in the remainder of the Late Cretaceous section has a typical austral affinity (e.g., Maud Rise and other circum-Antarctic sites) (Petrizzo, 2001).

Paleocene–Eocene

Sites 1135, 1136, and 1138 on the SKP and CKP (Figs. F1, F2) provide a relatively complete Paleocene and Eocene section of nannofossil-foraminifer oozes and chalks. An apparently complete Cretaceous/Tertiary boundary, in terms of assemblage succession, isotopic signature, and reworking of older (Cretaceous) nannofossil taxa, was recovered at Site 1138 (**Arney and Wise,** this volume). The boundary is marked by a significant color change, a negative carbon isotope shift, and a nannofossil turnover. As defined above, however, the boundary does not agree with available paleomagnetic data (Shipboard Scientific Party, 2000).

The Paleocene nannofossil assemblage is generally characteristic of high latitudes, and the Southern Ocean biogeography of *Hornibrookina* indicates a water mass boundary of some kind over the Kerguelen Plateau in the earliest Paleocene (**Arney and Wise,** this volume). This boundary disappeared by late Paleocene time, which is characterized by warm-water discoasters, sphenoliths, and fasciculiths. This documents relatively equable water temperatures during much of late Paleocene time, and preliminary floral and stable isotope analyses indicate that a reasonably complete record of the Late Paleocene Thermal Maximum (LPTM) was recovered at Site 1135 (**Arney and Wise,** this volume). At the beginning of middle Eocene time, water temperatures began to decline, nannofossil assemblages became dominated by cool-water species, and discoaster and sphenolith abundances and diversity were curtailed.

Eocene–Oligocene

High-latitude radiolarians from Site 1138 (Figs. F1, F2) reveal the Oligocene paleoceanographic history of the CKP (**Apel et al.,** this volume). Radiolarians are not preserved in Eocene sediments, but radiolarian preservation improves stepwise through Oligocene toward Miocene time, presumably linked to increased productivity triggered by climatic cooling (**Apel et al.,** this volume). Similar patterns of improving preservation across the Eocene/Oligocene boundary are observed in strata from other DSDP and ODP sites in the Southern Ocean. In contrast to the SKP, however, proxies for productivity are more complex at Site 1138. At the latter, carbonate dissolution is pronounced in the late Eocene–earliest Oligocene section, as indicated by poor preservation of foraminifers and common hiatuses. Radiolarian and diatom preservation, however, does not improve significantly until late early Oligocene time. Multiple measures of radiolarian diversity in Oligocene sediments from Site 1138 closely parallel radiolarian preservation, indicating that productivity controlled preserved radiolarian diversity (**Apel et al.,** this volume). Linear sedimentation rates, calculated from seven diatom bioevents spanning the early Oligocene to middle Miocene section, vary from 9.5 to 18 m/m.y., with an average of 12.6 m/m.y. (**Arney et al.,** this volume).

Site 1139, drilled on the flank of an eroded alkalic volcano, Skiff Bank (Figs. F1, F2), recovered mixed terrigenous-pelagic sediments of Oligocene and early Miocene age. Carbonate profiles through the interval show two prominent minima at ~28 and ~22 Ma that correspond to peaks in terrigenous flux (**Reusch,** this volume). These and higher-frequency variations of carbonate probably reflect glacio-eustatic/climatic changes, with glacial lowstands characterized by lower carbonate percentages, larger grain sizes, and higher opal concentrations. High Oligocene sedimentation rates of ~29 m/m.y. are attributed to high regional pelagic productivity plus the influx of fine terrigenous clastics derived from weathering of the exposed portions of Skiff Bank (**Persico and Wise,** this volume). A hostile terrestrial environment, lack of mineral surface area (silt vs. clay), and deposition below the oxygen minimum zone probably account for low organic carbon concentrations through the interval (**Reusch,** this volume). A paucity of clay suggests that physical as opposed to chemical weathering predominated, and it is likely that Skiff Bank experienced wave and ice erosion, especially during glacial times.

Miocene–Pleistocene

The ~300-m-thick Neogene section recovered at Site 1138 consists primarily of mixed carbonate and biosiliceous clay and ooze, with several thin (1–3 cm) tephra horizons and dispersed tephra (Coffin, Frey, Wallace, et al., 2000). Diatom biostratigraphic datums, supported by nannofossil and planktonic foraminifera biostratigraphy and $^{40}Ar/^{39}Ar$ ages from ash and tephra horizons, permit construction of a Neogene age-depth model (**Bohaty et al.,** this volume). A possible hiatus exists at the Oligocene/Miocene boundary, and a ~1 m.y. hiatus characterizes the Miocene/Pliocene boundary (**Bohaty et al.,** this volume; see also **Vigour and Lazarus,** this volume). The tephras at Site 1138 are glass rich, well sorted, and dominantly trachytic to rhyolitic in composition (**Bohaty et al.,** this volume). Volcaniclastic horizons are thought to have originated from Heard Island, ~180 km northwest of Site 1138, and were likely deposited both as primary ash fall and turbidites (**Bohaty et al.,** this volume).

Radiolarian assemblages of late middle Miocene to early Pliocene age are also well preserved at Site 1138 (Figs. **F1, F2**). Typical Antarctic faunas and consistently good preservation throughout the interval suggest that the site was located within the Antarctic radiolarian province and thus south of the Antarctic Polar Frontal Zone during the interval, which agrees with results from Site 747 to the south (**Vigour and Lazarus,** this volume). The distribution of other coarse-fraction components (e.g., sponge spicules and lithic fragments), suggests that dissolution, winnowing, and other benthic processes have not significantly affected the assemblages. Despite only moderate drilling recovery of the section, most lower to upper middle Pliocene radiolarian zones are present, although subzones could not be identified. **Vigour and Lazarus** (this volume) observed a significant discontinuity from 6.1 to 4.6 Ma but could not determine whether it was due to incomplete recovery of the section, to an interval of condensed sedimentation, or to a hiatus. Silicoflagellates are abundant and diverse in the Pliocene and Pleistocene sections, but some intervals of Miocene age at Site 1138 are barren or contain only limited numbers (**McCartney et al.,** this volume). As noted above, linear sedimentation rates calculated from diatom bioevents for the early Oligocene to middle Miocene interval average 12.6 m/m.y. (**Arney et al.,** this volume). At Site 1139 on Skiff Bank, significantly higher Miocene minimum sedimentation rates of ~18 m/m.y. may be explained by high regional pelagic productivity and fine terrigenous clastic input derived from exposed portions of the bank (Persico and Wise, this volume).

PALEOMAGNETISM AND ROCK MAGNETISM

New paleolatitudes for the CKP (Site 1138) and NKP (Site 1140) (Fig. F1) coincide with previous paleolatitudes obtained from Kerguelen Plateau and Ninetyeast Ridge rocks (Antretter et al., 2002). All of the paleolatitudes differ from one current option for the location of the Kerguelen hotspot at 49°S beneath the Kerguelen archipelago (Fig. F1). Motion between the Earth's mantle and rotation axis (i.e., true polar wander) cannot explain the difference. Numerical modeling of plume conduit motion in a large-scale mantle flow predicts southward motion of the Kerguelen hotspot of 3°–10°, which is consistent with paleomagnetic results (Antretter et al., 2002).

Igneous rocks from the seven Leg 183 basement sites (Figs. F1, F2) display variable rock magnetic properties (Zhao et al., this volume). Most subaerial basalt samples from Sites 1136, 1137, 1138, 1141, and 1142 underwent high-temperature oxidation deuterically, which is responsible for the high Curie temperature. These subaerial basalts are most likely good paleomagnetic recorders that preserve original and stable magnetic remanences. In contrast, basalt flows at Site 1139 underwent low-temperature oxidation. Substantial alteration at this site may have reset the original magnetization. At Site 1140, the fine grain size, inferred from rock magnetism, indicates rapid cooling of the pillow basalt samples. From the high-field magnetic moment curves and Curie points, it may be inferred that Ti-rich titanomagnetites are present in these submarine lavas, and they are expected to give accurate paleomagnetic results. Basalt recovered from Site 1142 was provisionally interpreted as pillow basalt in shipboard petrological descriptions. Results of rock magnetic investigations on a limited set of these rocks, however, suggest that they were most likely erupted in a subaerial environment, similar to their counterparts at Site 1141 (Zhao et al., this volume). The generally good magnetic stability and other properties exhibited by titanomagnetite-bearing rocks support the inference that the characteristic directions of magnetization isolated from Cretaceous rocks were acquired during the Cretaceous Normal Superchron (Shipboard Scientific Party, 2000). Thus, the stable inclinations obtained from these samples should be reliable for tectonic studies. Rock magnetic investigations of sediments from Sites 1138 and 1140 show that titanomagnetites with varying Ti content are the main magnetic minerals (Antretter et al., this volume).

Magnetic properties of subaerial and submarine basalts differ in opposite ways. In subaerial basalt, altered flow tops typically have high magnetic susceptibility and natural remanent magnetization (NRM) in the massive flow interiors, whereas submarine pillows and flows typically show the opposite (Delius et al., in press). Cooling and alteration are the main factors influencing the generation and distribution of oxide minerals, and the effects of low-temperature alteration are most noticeable in the distribution of more mobile elements (e.g., potassium). The main signal of the spectral gamma ray log is determined by potassium concentration and is therefore an excellent proxy for alteration. The strong positive correlation between total magnetic field and spectral gamma ray log response, both determined from downhole measurements, suggests that alteration can explain why submarine basalts show opposite magnetic properties to subaerial basalts (Delius et al., in press).

SUMMARY

We summarize results and interpretations in the context of the problems discussed in **"Scientific Objectives,"** p. 3.

1. Magmatism and Tectonics

a. New $^{40}Ar/^{39}Ar$ radiometric age determinations for all of the Leg 183 basement drill sites on the Kerguelen Plateau and Broken Ridge (Duncan, 2002), as well as for Leg 120 Site 750 (Coffin et al., 2002), comprise the best age control for any submarine LIP. Ages, in general, young northward on the Kerguelen Plateau, from ~119 to 120 Ma at Site 1136 in the south to ~34 to 35 Ma at Site 1140 in the north. The first age determinations of drilled igneous basement from Broken Ridge are ~94–95 Ma (Duncan, 2002). Combined with the above results and previous age determinations for basalt from the Ninetyeast Ridge (Duncan, 1978, 1991), new age determinations from basalt and lamprophyre attributed to the Kerguelen hotspot in India, Western Australia, and Antarctica (Coffin et al., 2002; Kent et al., 2002) make the ~130-m.y. record of Kerguelen hotspot activity the best documented of any hotspot trace on Earth. Paleolatitudes of Kerguelen Plateau and Ninetyeast Ridge basalt suggest 3°–10° southward motion of the hotspot relative to the rotation axis, a finding that can be modeled by large-scale mantle flow influencing the location of the plume conduit (Antretter et al., 2002).
b. Mafic crust totaling ~2.5×10^7 km^3 has been produced from the Kerguelen hotspot source(s) since ~130 Ma. Magma output has varied significantly through time, beginning with low volumes contemporaneous with or postdating continental breakup in Early Cretaceous time, extending through at least one and possibly two peaks in Early and Late Cretaceous time into a preexisting and growing ocean basin, and finally tapering to relatively steady state output in Late Cretaceous and Cenozoic time (Figs. **F3, F4**).
c. The 25-m.y. duration of peak hotspot output at geographically and tectonically diverse settings (Figs. **F3, F4**) is difficult to reconcile with current plume models. Coffin et al. (2002) propose two alternatives to the standard Hawaii model for hotspots, one involving multiple mantle plume sources and the other a single, but dismembered, plume source.

2. Petrogenesis

a. The uppermost igneous basement of the submarine Kerguelen Plateau is dominantly tholeiitic basalt. Except for some basalt units from Site 1140, incompatible element abundances distinguish the tholeiitic basalt forming the LIP from MORB (Fig. **F7**). However, alkalic basalt overlies tholeiitic basalt at Broken Ridge Site 1142 (Fig. **F5**) (Neal et al., 2002). An important exception to basaltic volcanism occurs at Site 1139, Skiff Bank on the NKP, where the igneous basement is a bimodal sequence of alkalic lavas ranging from trachybasalt to trachyte and rhyolite (Fig. F5), which is interpreted to be part of a shield volcano constructed on the basaltic plateau (Kieffer et al., 2002).

b. The uppermost basement lavas forming the LIP range widely in Sr, Nd, and Pb isotopic ratios, and each drill site has distinctive isotopic characteristics (Figs. F8, F9); differences in source materials and their proportions are inferred. Site 1140 basalt erupted within 50 km of the SEIR axis at 34 Ma, and the geochemical characteristics of Site 1140 lavas can be explained by mixing, in varying proportions, components derived from the Kerguelen plume and the source of SEIR MORB (Weis and Frey, 2002) (Figs. F8, F9). In contrast, like lavas from Site 738 on the SKP (Mahoney et al., 1995), lavas from Site 1137 on Elan Bank have radiogenic isotopic ratios that reflect a small and variable but significant role for continental crust in their petrogenesis (Weis et al., 2001; Ingle et al., 2002b) (Figs. F8, F9). The isotopic evidence indicating a role for continental crust correlates with a relative depletion in abundance of Nb (Fig. F10).

c. What was the origin and location of the continental components contributing to the LIP lavas? Intercalated within the basaltic flows at Site 1137 is a fluvial conglomerate with clasts of garnet-biotite gneiss containing zircon and monazite of Proterozoic age (Nicolaysen et al., 2001). This result shows that continental lithosphere, perhaps derived from the Eastern Ghats of eastern India for Site 1137 (Nicolaysen et al., 2001; Ingle et al., 2002a, 2002b), occurs at shallow depths within the Indian Ocean lithosphere. Although no evidence supports a continental component in Cenozoic lavas associated with the Kerguelen plume (i.e., basalt at Site 1140 and Kerguelen archipelago), these components are widely distributed in Cretaceous basalt forming the uppermost basement of the LIP. The most compelling examples are at Site 738 (SKP), Site 1137 (Elan Bank), and Site 747 (CKP) (Fig. F1) (Mahoney et al., 1995; Ingle et al., 2002b; and Frey et al., 2002b, respectively).

d. Basalts from Sites 747, 750, and 1139 are distinguished by unusually low $^{206}Pb/^{204}Pb$ ratios (<17.8) (Fig. F9). The origin of this low $^{206}Pb/^{204}Pb$ component may reflect a petrogenetic role for continental material, perhaps lower crust for Site 747 basalt (Frey et al., 2002a), but this component is quite different from the continental component contributing to basalt at Sites 738 and 1137 (Fig. F9).

e. A plume source, more complicated than a single plume head and stem model (Fig. F3), for the basalt forming the Kerguelen Plateau and Broken Ridge remains a viable hypothesis. Like the active plumes of Hawaii, Iceland, and the Galapagos, lavas forming the Kerguelen Plateau and Broken Ridge are isotopically heterogeneous. Difficult questions are to what extent is this heterogeneity intrinsic to the plume and to what extent does the heterogeneity reflect mixing between quite different components, such as depleted asthenosphere, oceanic lithosphere, and continental lithosphere. For lavas from some of the Kerguelen Plateau and Broken Ridge sites, the isotopic heterogeneity undoubtedly reflects mixing of plume-related components with components derived from depleted asthenosphere (Site 1140) or continental lithosphere (Sites 738, 747, and 1137).

Another important question is how the geochemical characteristics of the plume changed from ~120 to 24 Ma. For radiogenic isotopic ratios in lavas of varying age, aging is an obvious cause of heterogeneity. In a plot of initial $^{87}Sr/^{86}Sr$ vs. initial $^{143}Nd/^{144}Nd$, data for five sites (749, 1136, 1138, 1137, and 747) define a trend parallel to that defined by Kerguelen archipelago flood basalt (Fig. F8). The offset of the archipelago basalt data to higher ratios can largely be explained by aging of the mantle source from ~120–100 to 30–24 Ma, the age of archipelago flood basalt (see arrow in Fig. F8).

The effects of aging on Pb isotope ratios are more complex to evaluate because of the Pb isotopic diversity of Kerguelen Plateau and Broken Ridge lavas (Fig. F9). Undoubtedly, some of the diversity in Pb isotopic ratios reflects the sensitivity of Pb to components derived from continental crust. Three sites (747, 750, and 1139) have very low $^{206}Pb/^{204}Pb$ that cannot be related to the higher $^{206}Pb/^{204}Pb$ of the other LIP lavas by aging. Several sites (738, 1137, and, possibly, 1141/1142) have $^{207}Pb/^{204}Pb$ and $^{208}Pb/^{204}Pb$ ratios that have been increased by incorporation of continental components; consequently, it is difficult to evaluate radiogenic ingrowth of these ratios. Nevertheless, five sites (749, 1136, 1137, 1138, and 1141/42) have $^{206}Pb/^{204}Pb$ of ~18, approximately 0.2 to 0.6 lower than the archipelago basalt. As with the Sr and Nd isotopic ratios, the offset of these older lavas to lower $^{206}Pb/^{204}Pb$ may reflect radiogenic ingrowth in the source from ~120–100 to ~30–24 Ma; however, for reasonable $^{238}U/^{204}Pb$ ratios (<10) in the source this increase in $^{206}Pb/^{204}Pb$ is only <0.15 (see caption for Fig. F9). In summary, aging of the plume cannot account for most of the Pb isotopic differences between lavas forming the Cretaceous LIP and the Cenozoic Kerguelen archipelago (Fig. F9), but aging can account for the systematic offset in Sr and Nd isotopic ratios (Fig. F8).

3. Eruption Environment and Impact

a. Subsidence estimates for Site 1140 and other ODP drill sites indicate that the various parts of the Kerguelen Plateau subsided at a rate comparable to that for normal Indian Ocean lithosphere.
b. Sulfur release to Earth's atmosphere from 120 to 95 Ma, when the Southern and Central Kerguelen Plateau were constructed, could have had global climatic effects if the high latitude (low tropopause altitude) of the Kerguelen Plateau enabled powerful lava fountains to create convecting eruption plumes that reached the stratosphere. The previously unrecognized significant volume of explosive felsic volcanism that occurred when the Kerguelen Plateau and Broken Ridge were subaerial would have further contributed to the effects of this plume volcanism on global climate and environment.
c. Based on a decline in the seawater Sr isotopic evolution curve from ~122 to 112 Ma, submarine volcanism and hydrothermal activity as well as subaerial weathering and riverine transport during formation of the Kerguelen Plateau and Broken Ridge may also have had important effects on ocean chemistry.

d. Many of the subaerial lava flows recovered during Leg 183 drilling are of a type—rubbly pahoehoe—that appears to be distinct from slab and other recognized types of pahoehoe occurring in Hawaii. However, rubbly pahoehoe may be a common flow type in Iceland and the Columbia River Basalt Group.

4. Paleoenvironments and Paleoceanography

a. The CKP supported a dense conifer forest with various fern taxa and early angiosperms in late Albian to earliest Cenomanian time. By latest Cenomanian time, the CKP had subsided to a depth that allowed open marine sediments to accumulate. Cenomanian–Turonian time was warmer than subsequent Campanian–Maastrichtian time, when the paleoceanography of the CKP was characterized by little upwelling and a high degree of oxygenation. In contrast, by late Maastrichtian time, the northeast flank of the CKP was the site of significant upwelling and lower oxygenation.
b. An apparently complete Cretaceous/Tertiary boundary section at CKP Site 1138 is recognized by assemblage succession, isotopic signature, color change, and reworking of nannofossil taxa. A water mass boundary existed over the Kerguelen Plateau in earliest Paleocene time but had disappeared by late Paleocene time. A reasonably complete record of the Late Paleocene Thermal Maximum was recovered at Site 1135. At the beginning of middle Eocene time, water temperatures began to decline. Productivity of radiolarians increased in Oligocene time, presumably as water temperatures continued to decline. Sedimentation rates from early Oligocene to middle Miocene time vary from 9.5 to 18 m/m.y., averaging 12.6 m/m.y. Skiff Bank accumulated mixed terrigenous-pelagic sediments during Oligocene and early Miocene time, presumably related to glacioeustatic/climatic changes. By late middle Miocene to early Pliocene time, the CKP was south of the Antarctic Polar Frontal Zone.

ACKNOWLEDGMENTS

We thank reviewers V. Salters, A. Saunders, and P. Quilty for their constructive comments and G. Xu for preparation of geochemical figures. This synthesis is based on research accomplished by an international team of shipboard and shore-based scientists. None of this research could have been accomplished without the dedicated efforts of the ODP Operations Manager Mike Storms, SEDCO Drilling Superintendent Scott Pedersen, Captain Anthony Ribbens, and their respective ODP and SEDCO shipboard crews. This research used samples and data provided by the Ocean Drilling Program (ODP). The ODP is sponsored by the U.S. National Science Foundation (NSF) and participating countries under management of Joint Oceanographic Institutions (JOI), Inc. Funding for much of the Leg 183 research was provided by the U.S. Science Support Program (USSSP). University of Texas Institute for Geophysics Contribution 1606.

REFERENCES

Alibert, C., 1991. Mineralogy and geochemistry of a basalt from Site 738: implications for the tectonic history of the southernmost part of the Kerguelen Plateau. *In* Barron, J., Larsen, B., et al., *Proc. ODP, Sci. Results,* 119: College Station, TX (Ocean Drilling Program), 293–298.

Anderson, D.L., 1995. Lithosphere, asthenosphere, and perisphere. *Rev. Geophys.,* 33:125–149.

Andres, R.J., and Kasgnoc, A.D., 1998. A time-averaged inventory of subaerial volcanic sulfur emissions. *J. Geophys. Res.,* 103:25251–25261.

Antretter, M., Steinberger, B., Heider, F., and Soffel, H., 2002. Paleolatitudes of the Kerguelen hotspot: new paleomagnetic results and dynamic modeling. *Earth Planet. Sci. Lett.,* 203:635–650.

Artyushkov, E.V., Schlesinger, A.E., and Yanshin, A., 1980. The origin of vertical crustal movements within lithospheric plates. *In* Bally, A.W., Bender, P.L., McGetchin, T.R., and Walcott, R.I. (Eds.), *Dynamics of Plate Interiors.* Am. Geophys. Union, Geodyn. Ser., 1:37–51.

Baksi, A.K., 1995. Petrogenesis and timing of volcanism in the Rajmahal Flood-Basalt Province, northeastern India. *Chem. Geol.,* 121:73–90.

Barling, J., Goldstein, S.L., and Nicholls, I.A., 1994. Geochemistry of Heard Island (Southern Indian Ocean): characterization of an enriched mantle component and implications for enrichment of the sub-Indian Ocean Mantle. *J. Petrol.,* 35:1017–1053.

Barron, J., Larsen, B., et al., 1989. *Proc. ODP, Init. Repts.,* 119: College Station, TX (Ocean Drilling Program).

Beslier, M.-O., Le Bihan, T., Féraud, G., and Girardeau, J., 2001. Cretaceous ultra-slow spreading in the ocean–continent transition along the southwest Australian passive margin: constraints from ^{40}Ar/^{39}Ar dating. *Eur. Union Geosci. J. Conf. Abstr.,* 6:718.

Bonatti, E., 1990. Not so hot "hot spot" in the oceanic mantle. *Science,* 250:107–111.

Burke, K., 2001. Since 200 Ma nearly all large igneous provinces (LIPs) have been emplaced above deep mantle low velocity volumes (DMLVVS). *EOS, Trans. Am. Geophys. Union,* 82(F1134).

Campbell, I.H., and Griffiths, R.W., 1990. Implications of mantle plume structure for the evolution of flood basalts. *Earth Planet. Sci. Lett.,* 99:79–93.

Chand, S., Radhakrishna, M., and Subrahmanyam, C., 2001. India–East Antarctica conjugate margins: rift-shear tectonic setting inferred from gravity and bathymetry data. *Earth Planet. Sci. Lett.,* 185:225–236.

Coffin, M.F., 1992. Subsidence of the Kerguelen Plateau: the Atlantis concept. *In* Wise, S.W., Jr., Schlich, R., et al., *Proc. ODP, Sci. Results,* 120: College Station, TX (Ocean Drilling Program), 945–949.

Coffin, M.F., Davies, H.L., and Haxby, W.F., 1986. Structure of the Kerguelen Plateau province from SEASAT altimetry and seismic reflection data. *Nature,* 324:134–136.

Coffin, M.F., and Eldholm, O., 1994. Large igneous provinces: crustal structure, dimensions, and external consequences. *Rev. Geophys.,* 32:1–36.

Coffin, M.F., Pringle, M.S., Duncan, R.A., Gladczenko, T.P., Storey, R.D., Müller, R.D., and Gahagan, L.A., 2002. Kerguelen hotspot magma output since 130 Ma. *J. Petrol.,* 43:1121–1140.

Coleman, P.J., Michael, P.J., and Mutter, J.C., 1982. The origin of the Naturaliste Plateau, SE Indian Ocean: implications from dredged basalts. *J. Geol. Soc. Aust.,* 29:457–468.

Colwell, J.B., Symonds, P.A., and Crawford, A.J., 1994. The nature of the Wallaby (Cuvier) Plateau and other igneous provinces of the West Australian margin. AGSO *J. Aust. Geol. Geophys.,* 15:137–156.

Crough, S.T., 1983. The correction for sediment loading on the seafloor. *J. Geophys. Res.,* 88:6449–6454.

Damasceno, D., Scoates, J.S., Weis, D., Frey, F.A., and Giret, A., 2002. Mineral chemistry of mildly alkalic basalts from the 25 Ma Mont Crozier section, Kerguelen archipelago: constraints on phenocryst crystallization environments. *J. Petrol.,* 43:1389–1413.

Delius, H., Brewer, T.S., and Harvey, P.K., in press. Evidence for structural and alteration changes in basaltic lava flows using variation in magnetic rock properties (ODP Leg 183). *Tectonophysics.*

Detrick, R.S., Sclater, J.G., and Thiede, J., 1977. The subsidence of aseismic ridges. *Earth Planet. Sci. Lett.,* 34:185–198.

Doucet, S., Weis, D., Scoates, J.S., Nicolaysen, K., Frey, F.A., and Giret, A., 2002. The depleted mantle component in Kerguelen archipelago basalts: petrogenesis of tholeiitic-transitional basalts from the Loranchet Peninsula. *J. Petrol.,* 43:1341–1366.

Duncan, R.A., 1978. Geochronology of basalts from the Ninetyeast Ridge and continental dispersion in the eastern Indian Ocean. *J. Volcanol. Geotherm. Res.,* 4:283–305.

————, 1991. Age distribution of volcanism along aseismic ridges in the eastern Indian Ocean. *In* Weissel, J., Peirce, J., Taylor, E., Alt, J., et al., *Proc. ODP, Sci. Results,* 121: College Station, TX (Ocean Drilling Program), 507–517.

————, 2002. A time frame for construction of the Kerguelen Plateau and Broken Ridge. *J. Petrol.,* 43:1109–1120.

Duncan, R.A., and Clague, D.A., 1985. Pacific plate motion recorded by linear volcanic chains. *In* Nairn, A.E.M., Stehli, F.G., and Uyeda, S. (Eds.), *The Ocean Basins and Margins* (Vol. 7A): *The Pacific Ocean:* New York (Plenum), 89–121.

Duncan, R.A., and Storey, M., 1992. The life cycle of Indian Ocean hotspots. *In* Duncan, R.A., Rea, D.K., Kidd, R.B., von Rad, U., and Weissel, J.K. (Eds.), *Synthesis of Results from Scientific Drilling in the Indian Ocean.* Geophys. Monogr., Am. Geophys. Union, 70:91–103.

Eldholm, O., and Coffin, M.F., 2000. Large igneous provinces and plate tectonics. *In* Richards, M.A., Gordon, R.G., and van der Hilst, R.D. (Eds.), *The History and Dynamics of Global Plate Motions.* Am. Geophys. Union, Geophys. Monogr., 121:309–326.

Frey, F.A., Coffin, M.F., Wallace, P.J., Weis, D., Zhao, X., et al., 2000a. Origin and evolution of a submarine large igneous province: the Kerguelen Plateau and Broken Ridge, southern Indian Ocean. *Earth Planet. Sci. Lett.,* 176:73–89.

Frey, F.A., Dickey, J.S., Jr., Thompson, G., and Bryan, W.B., 1977. Eastern Indian Ocean DSDP sites: correlations between petrography, geochemistry and tectonic setting. *In* Heirtzler, J.R., Bolli, H.M., Davies, T.A., Saunders, J.B., and Sclater, J.G. (Eds.), *A Synthesis of Deep Sea Drilling in the Indian Ocean:* Washington (U.S. Govt. Printing Office), 189–257.

Frey, F.A., Jones, W.B., Davies, H., and Weis, D., 1991. Geochemical and petrologic data for basalts from Sites 756, 757, and 758: implications for the origin and evolution of the Ninetyeast Ridge. *In* Weissel, J., Peirce, J., Taylor, E., Alt, J., et al., *Proc. ODP, Sci. Results,* 121: College Station, TX (Ocean Drilling Program), 611–659.

Frey, F.A., McNaughton, N.J., Nelson, D.R., deLaeter, J.R., and Duncan, R.A., 1996. Petrogenesis of the Bunbury Basalt, Western Australia: interaction between the Kerguelen plume and Gondwana lithosphere? *Earth Planet. Sci. Lett.,* 144:163–183.

Frey, F.A., Nicolaysen, K., Kubit, B.K., Weis, D., and Giret, A., 2002a. Flood basalt from Mont Tourmente in the Central Kerguelen archipelago: the change from transitional to alkalic basalt at ~25 Ma. *J. Petrol.,* 43:1367–1388.

Frey, F.A., and Weis, D., 1995. Temporal evolution of the Kerguelen plume: geochemical evidence from ~38 to 82 Ma lavas forming the Ninetyeast Ridge. *Contrib. Mineral. Petrol.,* 121:12–28.

Frey, F.A., Weis, D., Borisova, A.Y., and Xu, G., 2002b. Involvement of continental crust in the formation of the Cretaceous Kerguelen Plateau: new perspectives from ODP Leg 120 sites. *J. Petrol.,* 43:1207–1240.

Frey, F.A., Weis, D., Yang, H.-J., Nicolaysen, K., Leyrit, H., and Giret, A., 2000b. Temporal geochemical trends in Kerguelen archipelago basalts: evidence for decreasing magma supply from the Kerguelen plume. *Chem. Geol.,* 164:61–80.

Gaina, C., Müller, R.D., Brown, B., and Ishihara, T., in press. Microcontinent formation around Australia. *In* Hillis, R., and Müller, R.D. (Eds.), *The Evolution and Dynamics of the Australian Plate*. Spec. Publ.—Jt. Geol. Soc. Aust./Am.

Garnero, E.J., 2000. Heterogeneity of the lowermost mantle. *Annu. Rev. Earth Planet. Sci.,* 28:509–537.

Gerlach, T.M., 1989. Degassing of carbon dioxide from basaltic magma at spreading centers: II, mid-oceanic ridge basalts. *J. Volcanol. Geotherm. Res.,* 39:221–232.

————, 1991. Present-day CO_2 emissions from volcanoes. *EOS, Trans. Am. Geophys. Union,* 72:249–255.

Gopala Rao, D., Krishna, K.S., and Sar, D., 1997. Crustal evolution and sedimentation history of the Bay of Bengal since the Cretaceous. *J. Geophys. Res.,* 102:17747–17768.

Harpp, K.S., and White, W.M., 2001. Tracing a mantle plume: isotopic and trace element variations of Galápagos seamounts. *Geochem. Geophys. Geosyst.,* 2 (Article), 10.1029/2000GC000137.

Hart, S.R., 1984. A large-scale isotope anomaly in the Southern Hemisphere mantle. *Nature,* 309:753–757.

Hayes, D.E., 1988. Age-depth relationships and depth anomalies in the Southeast Indian Ocean and South Atlantic Ocean. *J. Geophys. Res.,* 93:2937–2954.

Holbourn, A., and Kuhnt, W., 2002. Cenomanian–Turonian paleoceanographic change on the Kerguelen Plateau: a comparison with Northern Hemisphere records. *Cretaceous Res.,* 23:333–349.

Houtz, R.E., Hayes, D.E., and Markl, R.G., 1977. Kerguelen Plateau bathymetry, sediment distribution and crustal structure. *Mar. Geol.,* 25:95–130.

Ingle, S., Weis, D., Scoates, J., and Frey, F., 2002a. Indian continental crust sampled as pebbles within Elan Bank, Kerguelen Plateau (ODP Leg 183, Site 1137). *J. Petrol.,* 43:1241–1258.

————, 2002b. Relationship between the early Kerguelen plume and continental flood basalts of the paleo-Eastern Gondwana margin. *Earth Planet. Sci. Lett.,* 197:35–50.

Kempton, P.D., Fitton, J.G., Saunders, A.D., Nowell, G.M., Taylor, R.N., Hardarson, B.S., and Pearson, G., 2000. The Iceland plume in space and time: a Sr-Nd-Pb-Hf study of the North Atlantic rifted margin. *Earth Planet. Sci. Lett.,* 177:255–271.

Kent, R.W., Pringle, M.S., Müller, R.D., Saunders, A.D., and Ghose, N.C., 2002. $^{40}Ar/^{39}Ar$ geochronology of the Rajmahal basalts, India, and their relationship to the Kerguelen Plateau. *J. Petrol.,* 43:1141–1154.

Kent, R.W., Storey, M., and Saunders, A.D., 1992. Large igneous provinces: sites of plume impact or plume incubation? *Geology,* 20:891–894.

Kent, W., Saunders, A.D., Kempton, P.D., and Ghose, N.C., 1997. Rajmahal Basalts, eastern India: mantle sources and melt distribution at a volcanic rifted margin. *In* Mahoney, J.J., and Coffin, M.F. (Eds.), *Large Igneous Provinces: Continental, Oceanic and Planetary Flood Volcanism*. Geophys. Monogr., Am. Geophys. Union, 100:145–182.

Kieffer, B., Arndt, N.T., and Weis, D., 2002. A bimodal alkalic shield volcano on Skiff Bank: its place in the evolution of the Kerguelen Plateau. *J. Petrol.,* 43:1259–1286.

Larson, R.L., 1991. The latest pulse of Earth: evidence for a mid-Cretaceous superplume. *Geology,* 19:547–550.

Le Bas, M.J., Le Maitre, R.W., Streckeisen, A., and Zanettin, B., 1986. A chemical classification of volcanic rocks based on the total alkali-silica diagram. *J. Petrol.,* 27:745–750.

LeClaire, L., Bassias, Y., Denis-Clochiatti, M., Davies, H.L., Gautier, I., Gensous, B., Giannesini, P.-J., Patriat, P., Ségoufin, J., Tesson, M., and Wannesson, J., 1987. Lower Cretaceous basalt and sediments from the Kerguelen Plateau. *Geo-Mar. Lett.,* 7:169–176.

Macdonald, G.A., and Katsura, T., 1964. Chemical composition of Hawaiian lavas. *J. Petrol.,* 5:82–133.

Mahoney, J., Jones, W., Frey, F.A., Salters, V., Pyle, D., and Davies, H., 1995. Geochemical characteristics of lavas from Broken Ridge, the Naturaliste Plateau and southernmost Kerguelen Plateau: early volcanism of the Kerguelen hotspot. *Chem. Geol.,* 120:315–345.

Mahoney, J.J., Christie, D.M., Graham, D.W., Johnson, K.T.M., Hall, L.S., and Vonder-Haar, D.L., 2002. Between a hotspot and coldspot: isotopic variation in the Southeast Indian Ridge asthenosphere 86°E–118°E. *J. Petrol.,* 43:1155–1176.

Marzoli, A., Renne, P.R., Piccirilo, E.M., Ernesto, M., Bellieni, G., and De Min, A., 1999. Extensive 200-million-year-old continental flood basalts of the Central Atlantic Magmatic Province. *Science,* 284:616–618.

Mattielli, N., Weis, D., Blichert-Toft, J., and Albarede, F., 2002. Hf isotope evidence for a Miocene change in the Kerguelen mantle plume composition. *J. Petrol.,* 43:1327–1340.

McCormick, M.P., Thomason, L.W., and Trepte, C.R., 1995. Atmospheric effects of the Mt. Pinatubo eruption. *Nature,* 373:399–404.

McKenzie, D., and Sclater, J.G., 1971. The evolution of the Indian Ocean since the Late Cretaceous. *Geophys. J. R. Astron. Soc.,* 24:437–528.

Moore, J.G., 1970. Water content of basalt erupted on the ocean floor. *Contrib. Mineral. Petrol.,* 28:272–279.

Moore, J.G., and Fabbi, B.P., 1971. An estimate of the juvenile sulfur content of basalt. *Contrib. Mineral. Petrol.,* 33:118–127.

Morgan, W.J., 1971. Convection plumes in the lower mantle. *Nature,* 230:42–43.

Morgan, W.J., 1981. Hotspot tracks and the opening of the Atlantic and Indian Oceans. *In* Emiliani, C. (Ed.), *The Sea* (vol. 7): New York (Wiley-Interscience): 443–487.

Morgan, W.J., 1972. Deep mantle convection plumes and plate motions. *AAPG Bull.,* 56:203–213.

Müller, R.D., Gaina, C., Roest, W.R., and Hansen, D.L., 2001. A recipe for microcontinent formation. *Geology,* 29:203–206.

Müller, R.D., Royer, J.Y., and Lawver, L.A., 1993. Revised plate motions relative to the hotspots from combined Atlantic and Indian-Ocean hotspot tracks. *Geology,* 21:275–278.

Mutter, J.C., and Cande, S.C., 1983. The early opening between Broken Ridge and Kerguelen Plateau. *Earth Planet. Sci. Lett.,* 65:369–376.

Neal, C.R., Mahoney, J.J., and Chazey, W.J., 2002. Mantle sources and the highly variable role of continental lithosphere in basalt petrogenesis of the Kerguelen Plateau and Broken Ridge LIP: results from Ocean Drilling Program Leg 183. *J. Petrol.,* 43:1177–1206.

Nicolaysen, K., Bowring, S., Frey, F., Weis, D., Ingle, S., Pringle, M.S., Coffin, M.F., and the Leg 183 Shipboard Scientific Party, 2001. Provenance of Proterozoic garnet-biotite gneiss recovered from Elan Bank, Kerguelen Plateau, southern Indian Ocean. *Geology,* 29:235–238.

Nicolaysen, K., Frey, F.A., Hodges, K.V., Weis, D., and Giret, A., 2000. ^{40}Ar/^{39}Ar geochronology of flood basalts from the Kerguelen archipelago, southern Indian Ocean: implication for Cenozoic eruption rates of the Kerguelen plume. *Earth Planet. Sci. Lett.*, 174:318–328.

Olson, P., 1990. Hot spots, swells and mantle plumes. *In* Ryan, M.P. (Ed.), *Magma Transport and Storage:* London (Wiley and Sons), 33–51.

Petrizzo, M.R., 2001. Late Cretaceous planktonic foraminifera from the Kerguelen Plateau (ODP Leg 183): new data to improve the Southern Oceans biozonation. *Cretaceous Res.,* 22:829–855.

Pringle, M., Nicolaysen, K., Lee, M.R., and Parsons, I., 2000. Ar/Ar and U/Pb ages of felsic igneous clasts recovered from ODP Site 1137, Kerguelen Plateau, southern Indian Ocean. *EOS, Trans. Am. Geophys. Union,* 81:S432.

Pringle, M.S., Storey, M., and Wijbrans, J., 1994. $^{40}Ar/^{39}Ar$ geochronology of mid-Cretaceous Indian ocean basalts: constraints on the origin of large flood basalt. *Eos,* 75:728.

Pyle, D.M., Beattie, P.D., and Bluth, G.J.S., 1996. Sulphur emissions to the stratosphere from explosive volcanic eruptions. *Bull. Volcan.,* 57:663–671.

Quilty, P.G., Shafik, S., McMinn, A., Brady, H., and Clarke, I., 1983. Microfossil evidence for the age and environment of deposition of sediments of Heard and McDonald Islands. *In* Oliver, R.L., James, P.R., and Jago, J.B. (Eds.), *Antarctic Earth Science.* Aust. Acad. Sci., Canberra, 636–639.

Quilty, P.G., and Wheller, G., 2000. Heard Island and the McDonald Island: a window into the Kerguelen Plateau. *Pap. Proc. R. Soc. Tasmania,* 133:1–12.

Retallack, G.J., 2001. A 300 million-year record of atmospheric carbon dioxide from fossil plant cuticles. *Nature,* 411:287–290.

Roeser, H.A., Fritsch, J., and Hinz, K., 1996. The development of the crust off Dronning Maud Land, East Antarctica. *In* Storey, B.C., King, E.C., and Livermore, R.A. (Eds.), *Weddell Sea Tectonics and Gondwana Break-up.* Spec. Publ.—Geol. Soc. London, 108:243–264.

Saunders, A., Storey, M., Kent, R.W., and Gibson, I.L., 1994. Magmatic actvity associated with the Kerguelen-Heard plume: implications for plume dynamics. *Mem. Soc. Geol. Fr.,* 166:61–72.

Saunders, A.D., Storey, M., Gibson, I.L., Leat, P., Hergt, J., and Thompson, R.N., 1991. Chemical and isotopic constraints on the origin of basalts from Ninetyeast Ridge, Indian Ocean: results from DSDP Legs 22 and 26 and ODP Leg 121. *In* Weissel, J., Peirce, J., Taylor, E., Alt, J., et al., *Proc. ODP, Sci. Results,* 121: College Station, TX (Ocean Drilling Program), 559–590.

Saunders, A.D., Storey, M., Kent, R.W., and Norry, M.J., 1992. Consequences of plume-lithosphere interactions. *In* Storey, B.C., Alabaster, T., and Pankhurst, R.J. (Eds.), *Magmatism and the Causes of Continental Break-up.* Spec. Publ.—Geol. Soc. London, 68:41–60.

Scaillet, B., Clemente, B., Evans, B.W., and Pichavant, M., 1998. Redox control of sulfur degassing in silicic magmas. *J. Geophys. Res.* 103:23937–23949.

Schilling, J.G., Bergeron, M.B., and Evans, R., 1980. Halogens in the mantle beneath the North Atlantic. *Philos. Trans. R. Soc. London, Ser. A,* 297:147–178.

Schlich, R., Wise, S.W., Jr., et al., 1989. *Proc. ODP, Init. Repts.,* 120: College Station, TX (Ocean Drilling Program).

Self, S., Keszthelyi, L., and Thordarson, T., 1998. The importance of pahoehoe. *Annu. Rev. Earth Planet. Sci,* 26:81–110.

Shipboard Scientific Party, 2000. Leg 183 summary: Kerguelen Plateau–Broken Ridge—A large igneous province. In Coffin, M.F., Frey, F.A., Wallace, P.J., et al., *Proc. ODP, Init. Repts.,* 183: College Station, TX (Ocean Drilling Program), 1–101.

Sleep, N.H., 1996. Lateral flow of hot plume material ponded at sublithospheric depths. *J. Geophys. Res.,* 101:28065–28083.

————, 1997. Lateral flow and ponding of starting plume material. *J. Geophys. Res.,* 102:10001–10012.

Stagg, H.M.J., 1985. The structure and origin of Prydz Bay and MacRobertson Shelf, East Antarctica. *Tectonophysics,* 114:315–340.

Stein, M., and Hofmann, A.W., 1994. Mantle plumes and episodic crustal growth. *Nature,* 373:63–68.

Steinberger, B., and O'Connell, R.J., 1998. Advection of plumes in mantle flow: implications for hotspot motion, mantle viscosity and plume distribution. *Geophys. J. Int.,* 132:412–434.

Storey, B.C., 1995. The role of mantle plumes in continental breakup: case histories from Gondwanaland. *Nature,* 377:301–308.

Storey, M., Kent, R.W., Saunders, A.D., Salters, V.J., Hergt, J., Whitechurch, H., Sevigny, J.H., Thirlwall, M.F., Leat, P., Ghose, N.C., and Gifford, M., 1992. Lower Cretaceous volcanic rocks on continental margins and their relationship to the Kerguelen Plateau. *In* Wise, S.W., Jr., Schlich, R., et al., *Proc. ODP, Sci. Results,* 120: College Station, TX (Ocean Drilling Program), 33–53.

Storey, M., Saunders, A.D., Tarney, J., Gibson, I.L., Norry, M.J., Thirlwall, M.F., Leat, P., Thompson, R.N., and Menzies, M.A., 1989. Contamination of Indian Ocean asthenosphere by the Kerguelen-Heard mantle plume. *Nature,* 338:574–576.

Stothers, R.B., Wolff, J.A., Self, S., and Rampino, M.R., 1986. Basaltic fissure eruptions, plume heights, and atmospheric aerosols. *Geophys. Res. Lett.,* 13:725–728.

Subrahmanyam, C., Thakur, N.K., Gangadhara Rao, T., Khanna, R., Ramana, M.V., and Subrahmanyam, V., 1999. Tectonics of the Bay of Bengal: new insights from satellite-gravity and shipborne geophysical data. *Earth Planet. Sci. Lett.,* 171:237–251.

Sun, S.-S., and McDonough, W.F., 1989. Chemical and isotopic systematics of oceanic basalts: implications for mantle composition and processes. *In* Saunders, A.D., and Norry, M.J. (Eds.), *Magmatism in the Ocean Basins.* Spec. Publ.—Geol. Soc. London, 42:313–345.

Symonds, P.A., Planke, S., Frey, Ø., and Skogseid, J., 1998. Volcanic development of the Western Australian continental margin and its implications for basin development. *In* Purcell, P.G., and Purcell, R.R. (Eds.), *The Sedimentary Basins of Western Australia,* 2: Perth, Australia (Petrol. Exp. Soc. Aust.), 33–54.

Tejada, M.L.G., Mahoney, J.J., Duncan, R.A., and Hawkins, M.P., 1996. Age and geochemistry of basement and alkalic rocks of Malaita and Santa Isabel, Solomon Islands, southern margin of the Ontong Java Plateau. *J. Petrol.* 37:361–394.

Thompson, R.N., and Gibson, S.A., 1991. Subcontinental mantle plumes, hotspots and pre-existing thinspots. *J. Geol. Soc. London,* 147:973–977.

Unni, C.K., and Schilling, J.G., 1978. Cl and Br degassing by volcanism along the Reykjanes Ridge and Iceland. *Nature,* 272:19–23.

Varekamp, J.C., Kreulen, R., Poorter, R.P.E., and Van Bergen, M.J., 1992. Carbon sources in arc volcanism, with implications for the carbon cycle. *Terra Nova,* 4:363–373.

Wallace, P., 2001. Volcanic SO_2 emissions and the abundance and distribution of exsolved gas in magmas. *J. Volcanol. Geotherm. Res.,* 108:85–106.

Wallace, P., Cervantes, P., Weis, D., Ingle, S., Frey, F.A., Kieffer, B., and Moore, C.L., 2000. Explosive felsic volcanism on the Kerguelen Plateau (ODP Leg 183): geochemical characteristics and pre-eruptive volatile contents. *EOS, Trans. Am. Geophys. Union,* 81:432.

Wallace, P.J., 2002. Volatiles in submarine basaltic glasses from the Northern Kerguelen Plateau (ODP Site 1140): implications for source region compositions, shallow magmatic processes and plateau subsidence. *J. Petrol.,* 43:1311–1326.

Weis, D., and Frey, F.A., 2002. Submarine basalts of the Northern Kerguelen Plateau: interaction between the Kerguelen Plume and the Southeast Indian Ridge revealed at ODP Site 1140. *J. Petrol.,* 43:1287–1310.

Weis, D., Frey, F.A., Giret, A., and Cantagrel, J.M., 1998. Geochemical characteristics of the youngest volcano (Mount Ross) in the Kerguelen archipelago: inferences for magma flux and composition of the Kerguelen plume. *J. Petrol.,* 39:973–994.

Weis, D., Frey, F.A., Leyrit, H., and Gautier, I., 1993. Kerguelen archipelago revisited: geochemical and isotopic study of the Southeast Province lavas. *Earth Planet. Sci. Lett.,* 118:101–119.

Weis, D., Frey, F.A., Saunders, A., Gibson, I.L., Dehn, J., Driscoll, N., Farrell, J., Fourtanier, E., Gamson, P.D., Gee, J.S., Janecek, T., Klootwijk, C., Lawrence, J.R., Littke, R., Newman, J.S., Nomura, R., Owen, R.M., Peirce, J., Popsichal, J.J., Rea, D.K., Resiwati, P., Smit, J., Smith, G.M., Tamaki, K., Taylor, E., Weissel, J., and Wilkinson, C., 1991. Ninetyeast Ridge (Indian Ocean): a 5000 km record of a Dupal mantle plume. *Geology,* 19:99–102.

Weis, D., Frey, F.A., Schlich, R., Schaming, M., Montigny, R., Damasceno, D., Mattielli, N., Nicolaysen, K.E., and Scoates, J.S., 2002. Trace of the Kerguelen mantle plume: evidence from seamounts between the Kerguelen archipelago and Heard Island, Indian Ocean. *Geochem. Geophys. Geosystems,* 3 (Article), 10.1029/2001GC000251.

Weis, D., and Giret, A., 1994. Kerguelen plutonic complexes: Sr, Nd, Pb isotopic study and inferences about their sources, age, and geodynamic setting. *Bull. Soc. Geol. France,* 166:47–59.

Weis, D., Ingle, S., Damasceno, D., Frey, F.A., Nicolaysen, K., and Barling, J., 2001. Origin of continental components in Indian Ocean basalts: evidence from Elan Bank (Kerguelen Plateau, ODP Leg 183, Site 1137). *Geology,* 29:147–150.

White, R.S., 1993. Melt production rates in mantle plumes. *Philos. Trans. R. Soc. London, Ser. A,* 342:137–153.

White, R.S., and McKenzie, D., 1989. Magmatism at rift zones: the generation of volcanic continental margins and flood basalts. *J. Geophys. Res.,* 94:7685–7729.

————, 1995. Mantle plumes and flood basalts. *J. Geophys. Res.,* 100:17543–17585.

Whitechurch, H., Montigny, R., Sevigny, J., Storey, M., and Salters, V.J.M., 1992. K-Ar and ^{40}Ar ages of central Kerguelen Plateau basalts. *In* Wise, S.W., Jr., Schlich, R., et al., *Proc. ODP, Sci. Results,* 120: College Station, TX (Ocean Drilling Program), 71–77.

Wilson, J.T., 1963. A possible origin of the Hawaiian Islands. *Can. J. Phys.,* 41:863–870.

————, 1965. Evidence from ocean islands suggesting movement in the Earth. *Philos. Trans. R. Soc. London, Ser. A,* 258:145–167.

Wilson, L., Sparks, R.S.J., and Walker, G.P.L., 1980. Explosive volcanic eruptions IV. The control of magma properties and conduit geometry on eruption column behaviour. *Geophys. J. R. Astron. Soc.,* 63:117–148.

Wilson, M., and Patterson, R., 2001. Intra-plate magmatism related to hot fingers in the upper mantle: evidence from the Tertiary–Quaternary volcanic province of western and central Europe. *In* Ernst, R., and Buchan, K. (Eds.), *Mantle Plumes: Their Identification through Time.* Spec. Publ.—Geol. Soc. Am., 352:37–58.

Yang, H.-J., Frey, F.A., Weis, D., Giret, A., Pyle, D., and Michon, G., 1998. Petrogenesis of the flood basalts forming the northern Kerguelen archipelago: implications for the Kerguelen plume. *J. Petrol.,* 39:711–748.

Figure F1. Basalt provinces in the eastern Indian Ocean. Oceanic features attributed to the Kerguelen plume include the Kerguelen Plateau, Broken Ridge, Ninetyeast Ridge, Kerguelen archipelago, and Heard and McDonald Islands. Several continental basalt provinces have also been associated with the Kerguelen plume; these include Cretaceous lamprophyres in Antarctica and northeast India (solid diamonds), the Rajmahal Traps in northeast India, and Bunbury Basalt (BB) in Southwest Australia. Solid circles = locations of igneous basement sites drilled by DSDP and ODP, open circle = *Eltanin* piston core. Also indicated are dredge locations (solid squares = igneous rock recovery, open square = sediment dredge by *Petuna Explorer*). NKP, CKP and SKP = northern, central, and southern Kerguelen Plateau, respectively.

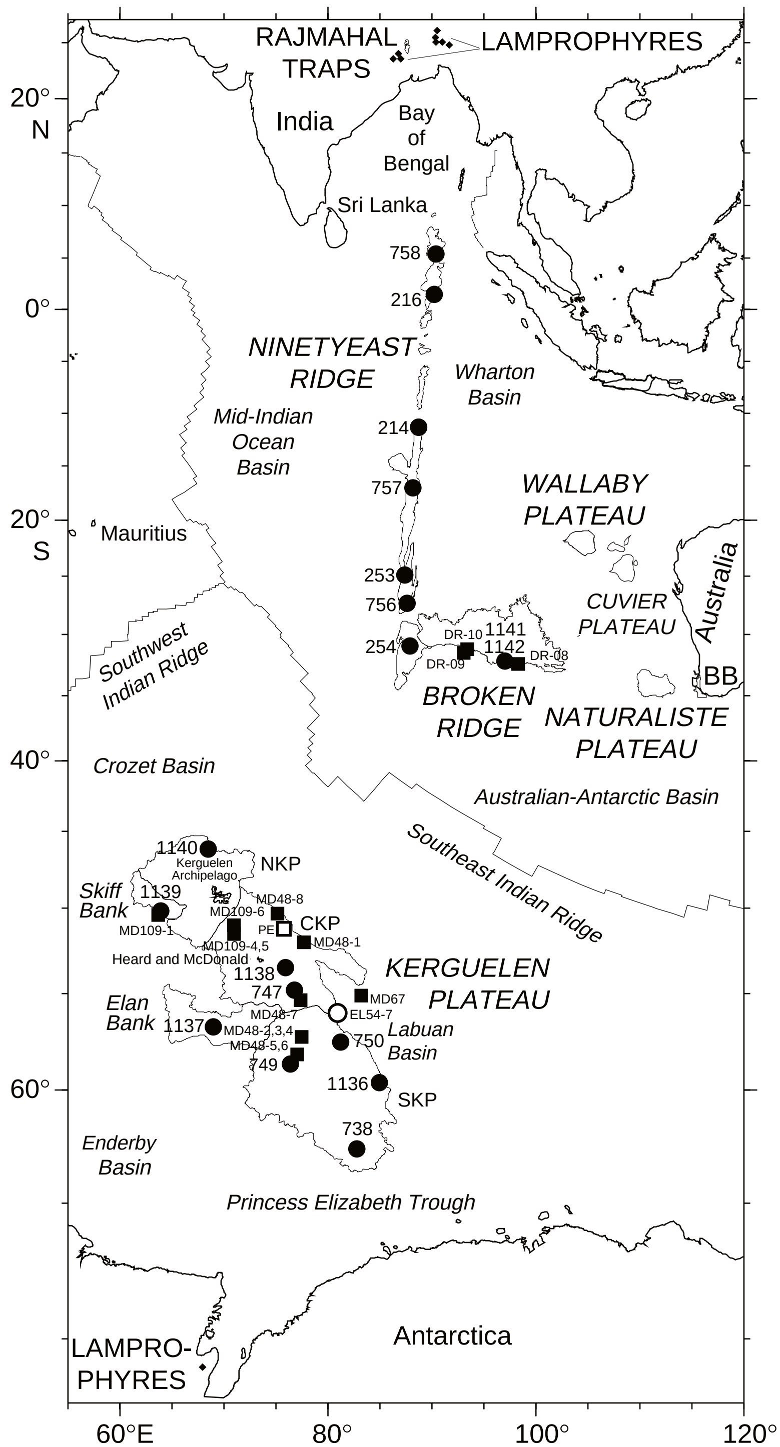

Figure F2. Summary of ODP drill holes on the Kerguelen Plateau and Broken Ridge that recovered volcanic rocks from the uppermost igneous basement (see Fig. **F1**, p. 36, for locations). Data for Leg 183 (Sites 1136, 1137, 1138, 1139, 1140, 1141, and 1142) are from Coffin, Frey, Wallace, et al. (2000), Coffin et al. (2002), and Duncan (2002). Data for other sites are from Barron, Larsen, et al. (1989), and Schlich, Wise, et al. (1989). Radiometric ages ($^{40}Ar/^{39}Ar$) for mafic volcanics are in bold.

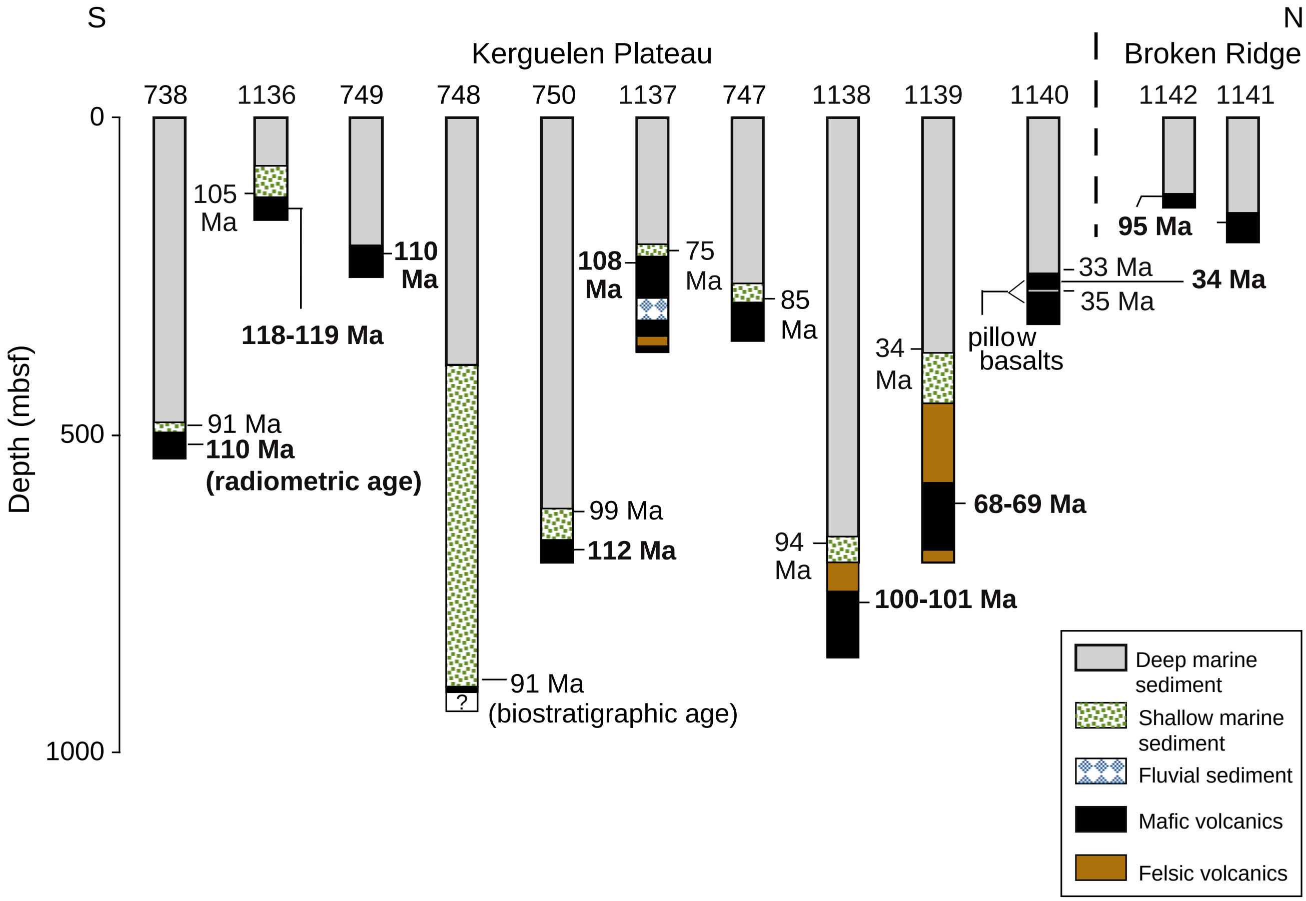

Figure F3. Estimated Kerguelen hotspot magma output since ≈130 Ma (Coffin et al., 2002). Analytical uncertainties for $^{40}Ar/^{39}Ar$ ages are variable, but 2-σ values are generally <5 m.y. Therefore, ages were assigned to various portions of the province (Fig. **F1,** p. 36) in 5-m.y. bins (diamonds) for the purpose of calculating the hotspot magma flux. The dashed line between 95 and 85 Ma indicates assumed Ninetyeast Ridge crust of that age buried beneath the Bengal Fan, produced at the same rate as Ninetyeast Ridge and Skiff Bank crust from 85 to 35 Ma.

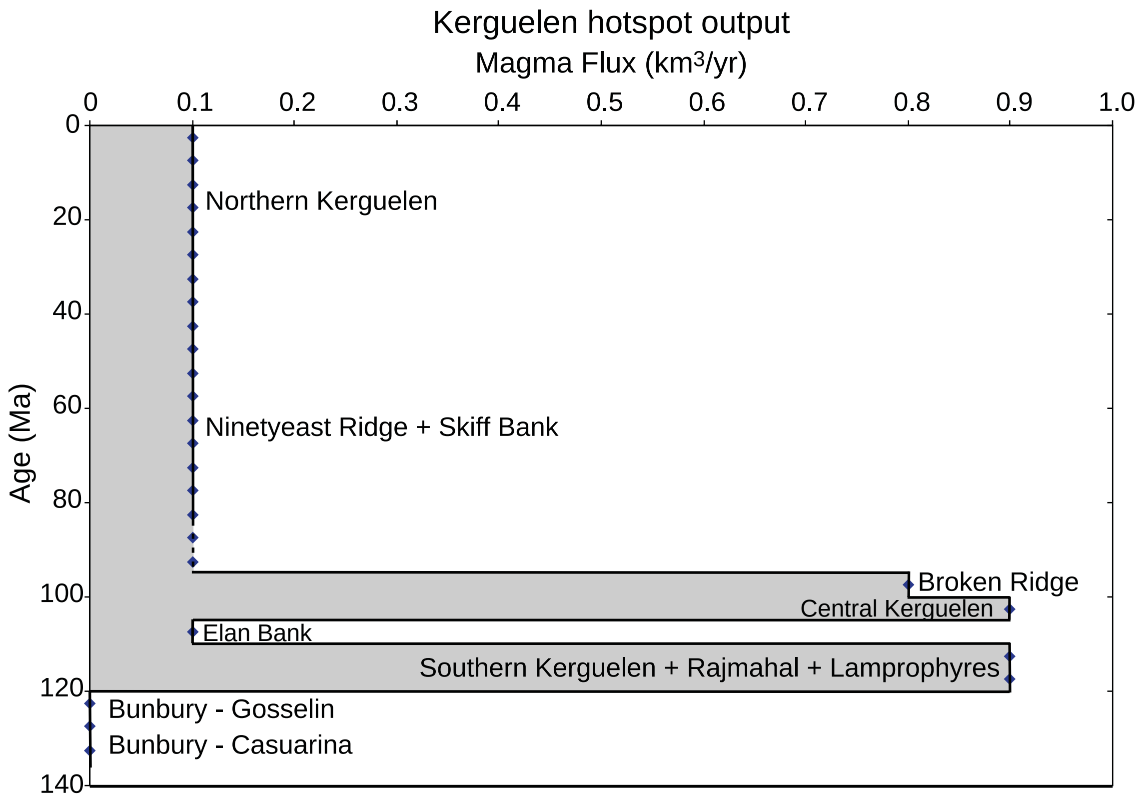

Figure F4. Plate reconstructions of the southern Indian Ocean region of Coffin et al. (2002), using the hotspot reference frame of Müller et al. (1993). Red stars = possible reconstructed positions of the Kerguelen hotspot (after Müller et al., 1993); those labeled "K" assume that the Kerguelen archipelago is the current location of the Kerguelen hotspot, and those labeled "H" assume that Heard Island is the hotspot's current location. Black shading = magmatism associated with the Kerguelen hotspot, diamonds = lamprophyres (labeled with "L" in 110 Ma panel) as they have appeared through geologic time (see Fig. F1, p. 36, for current locations of individual igneous complexes). Dashed line = a possible northern boundary for Greater India. IND = India, ANT = Antarctica, AUS = Australia. **A, B.** Seafloor spreading initiated at ~133 Ma between Western Australia and Greater India and at ~125 Ma between Australia and Antarctica. This model assumes breakup between India and Antarctica at ~133 Ma, although the timing of this event is not well known. The Bunbury Basalt (BB) of Southwest Australia erupted close to these breakup events in both time and space. Continental portions of Elan Bank (EB) and the Southern Kerguelen Plateau (unknown dimensions) remained attached to Greater India at these times. The Naturaliste Plateau (NP) also contains continental crust. **C, D.** Seafloor spreading continued between India, Antarctica, and Australia. The initial massive pulse of Kerguelen magmatism created the Southern Kerguelen Plateau (SKP), the Rajmahal Traps (RAJ), and Indian/Antarctic lamprophyres (L) from ~120 to ~110 Ma (Fig. F3, p. 38) and may be linked to breakup and separation between Elan Bank and Greater India. The Central Kerguelen Plateau (CKP) formed between ~105 and ~100 Ma and Broken Ridge (BR) between ~100 and ~95 Ma (Fig. F3, p. 38). Igneous basement of the Wallaby Plateau (WP) is not well characterized geochemically and has not been dated, but its age is inferred to lie between ~120 and ~100 Ma (Colwell et al., 1994). (Continued on next page.)

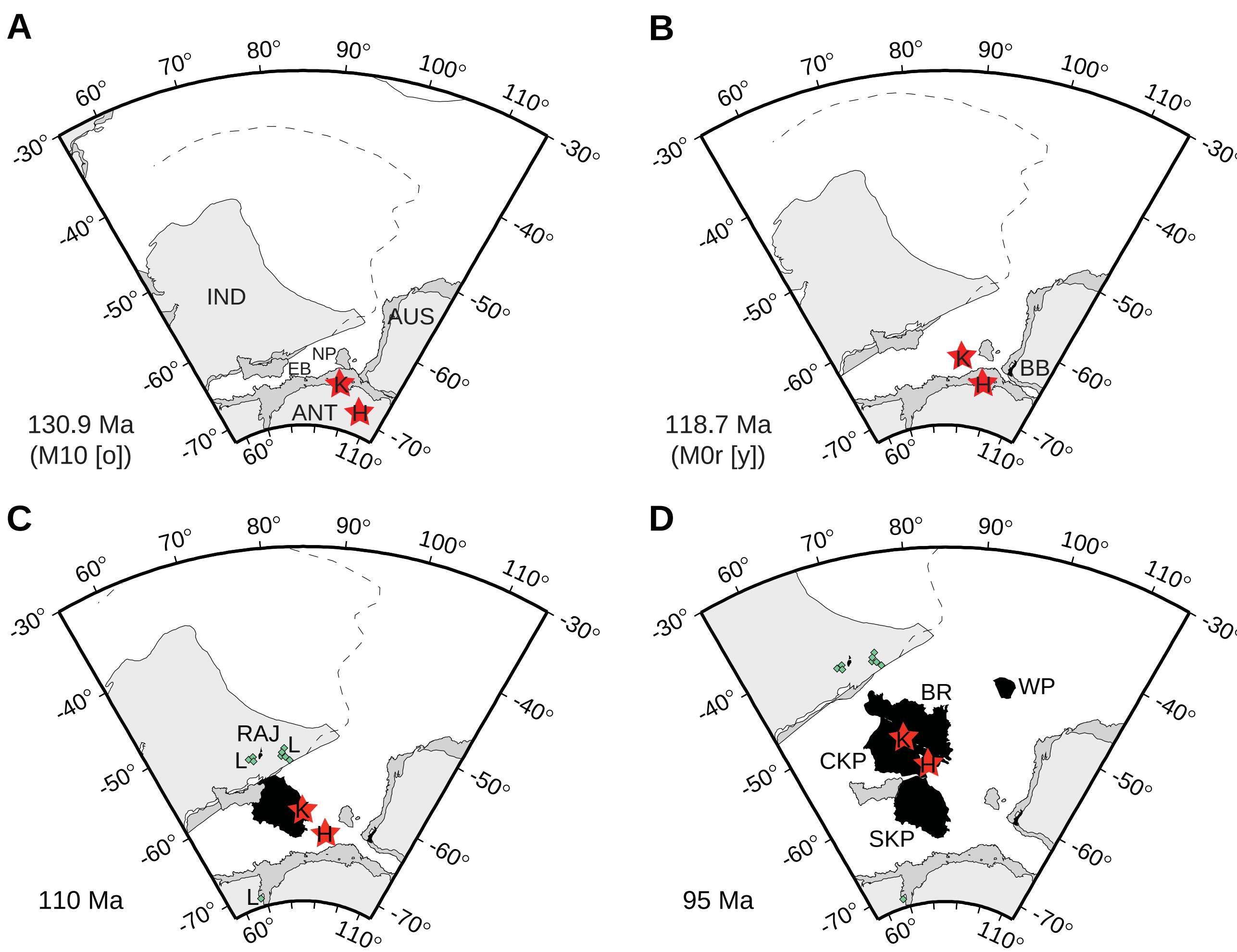

Figure F4 (continued). E, F. The hotspot generated the Ninetyeast Ridge (NER) and Skiff Bank (SB) as India continued its northward drift relative to Antarctica. **G, H.** At ~40 Ma, seafloor spreading commenced between the Central Kerguelen Plateau and Broken Ridge. The hotspot generated the Northern Kerguelen Plateau (NKP), and, since 40 Ma, as Broken Ridge and the Kerguelen Plateau have continued to separate, has produced the Kerguelen archipelago, Heard and McDonald Islands (Fig. **F1,** p. 36), and the chain of volcanoes between Kerguelen and Heard (Weis et al., 2002).

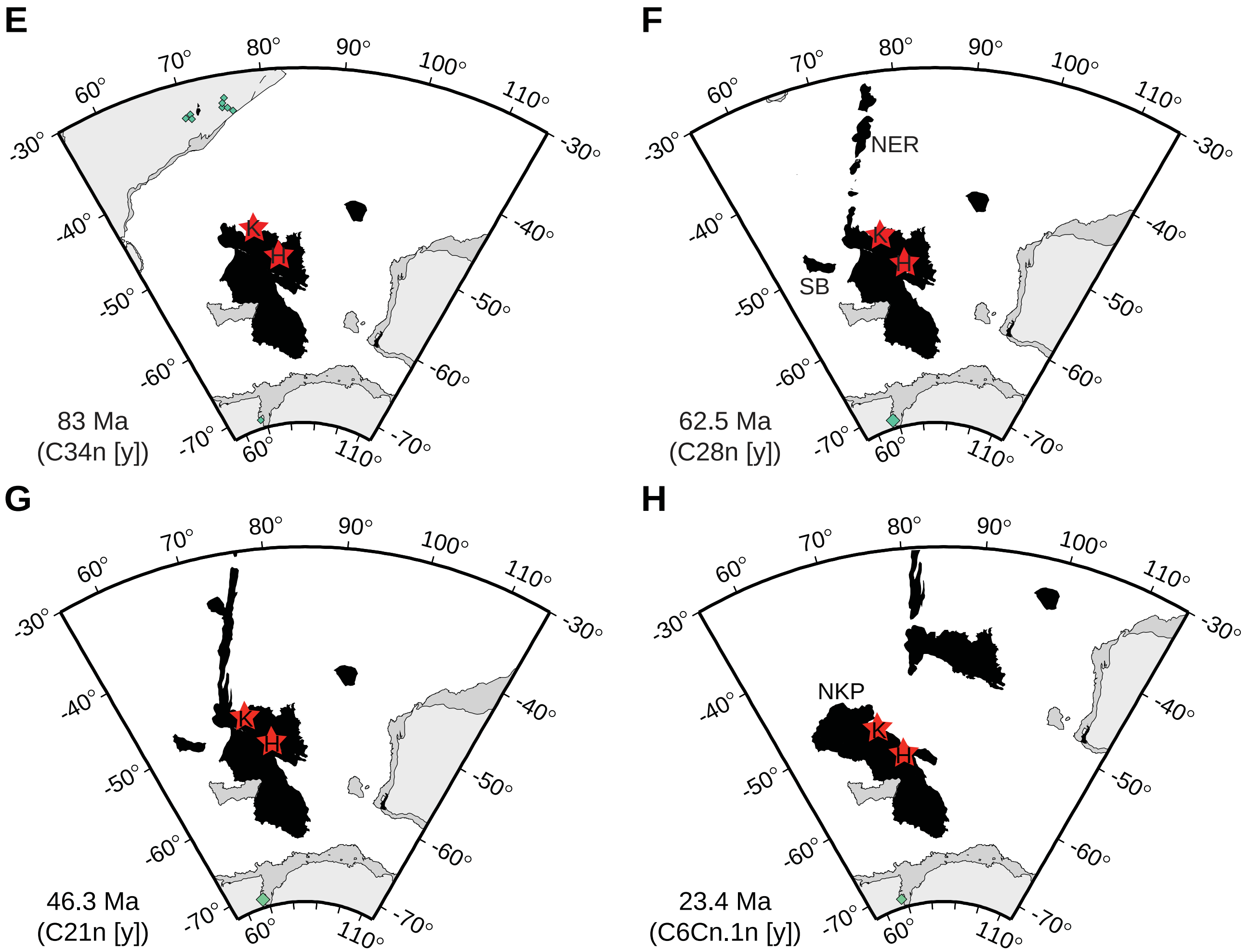

Figure F5. Total alkalis vs. SiO_2 classification plot (Le Bas et al., 1986) for igneous basement rocks recovered during Leg 183. Data sources are Neal et al. (2002) for Sites 1136, 1138, 1141, and 1142; Ingle et al. (2002a, 2002b) for Site 1137; Kieffer et al. (2002) for Site 1139; and Weis and Frey (2002) for Site 1140. Solid triangles = samples of volcanic rock that occur as clasts in the Site 1137 fluvial sediments. All data were obtained by X-ray fluorescence at the University of Massachusetts, Amherst. Only samples with loss on ignition <5 wt% are plotted, and Fe^{2+} is calculated as 85% of the total iron. The dividing line between alkalic and tholeiitic basalt is from Macdonald and Katsura (1964). Important features are (a) the dominance of tholeiitic basalt at Sites 1136 and 1140; (b) basalts from Sites 1137 and 1138 straddle the alkalic/tholeiitic boundary line; (c) igneous clasts in the conglomerate at Site 1137 have diverse compositions ranging from phonotephrite to trachyte and rhyolite; based on $^{40}Ar/^{39}Ar$ data the ages of these felsic igneous clasts are indistinguishable from the ages of the Site 1137 basalt flows (Pringle et al., 2000); (d) the occurrence of a bimodal alkalic suite, trachybasalt to rhyolite, at Site 1139; and (e) most of the basalts at Sites 1141 and 1142 are slightly alkalic; the trachybasalt is a clast in Unit 2 breccia, and the tholeiitic basaltic andesite is from Unit 6 at Site 1142.

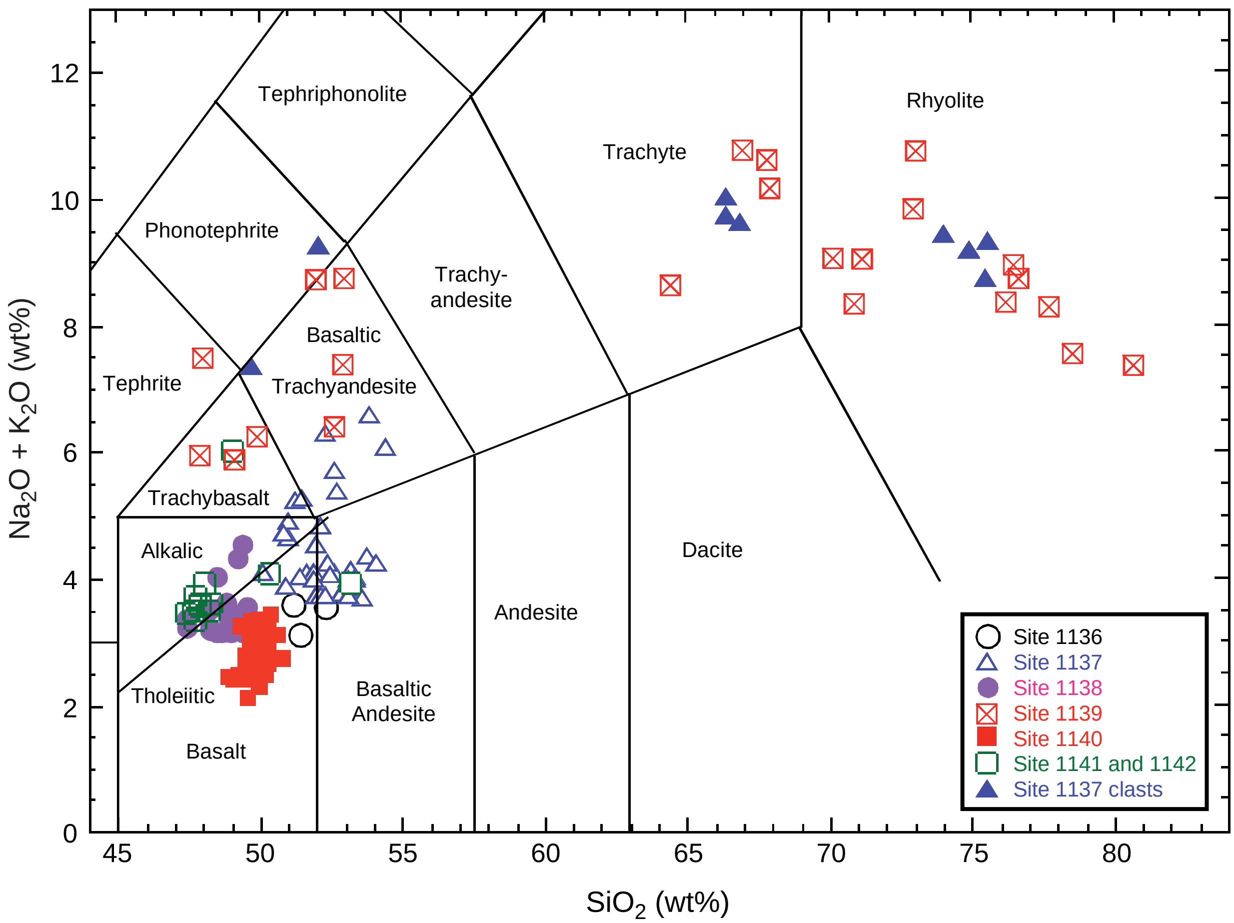

Figure F6. Abundance of TiO_2 vs. MgO for basement igneous rocks recovered during Leg 183. Data sources are Neal et al. (2002) for Sites 1136, 1138, 1141, and 1142; Ingle et al. (2002a, 2002b) for Site 1137; Kieffer et al. (2002) for Site 1139; and Weis and Frey (2002) for Site 1140. Important features are (a) the wide range in MgO content with many of the clasts in the conglomerate at Site 1137 and several samples at Site 1139 containing <1 wt% MgO and (b) Site 1140 lavas define three subparallel trends, which reflect units containing varying proportions of MORB- and plume-related components.

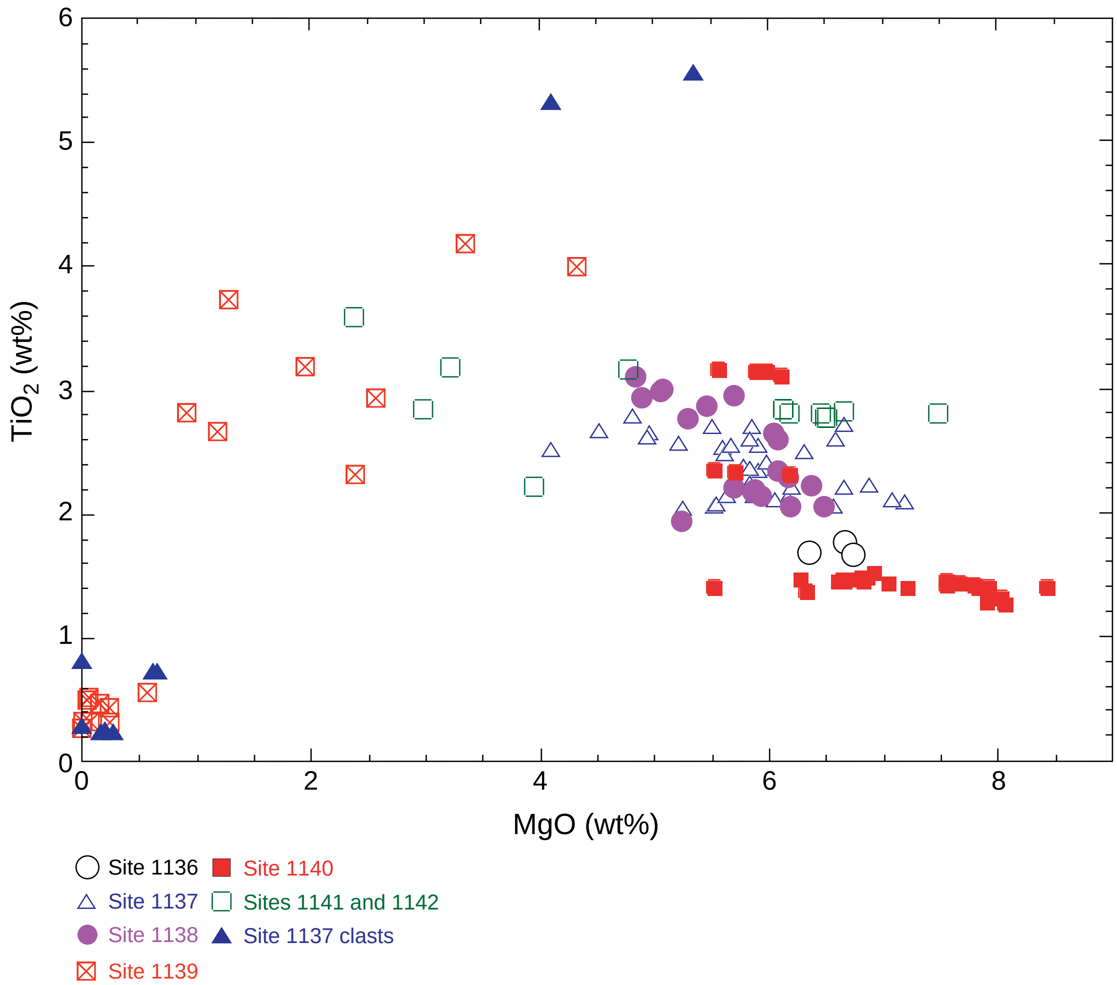

Figure F7. Incompatible element abundances in basaltic samples (MgO ranges from ~4.3 to 7.5 wt%) representing distinctive units from each drill hole normalized to primitive mantle (PM) abundances (Sun and McDonough, 1989); note vertical scale is linear. From right to left the elements are increasingly more incompatible in basalt and peridotite mineral assemblages. Data sources are Mahoney et al. (1995), Frey et al. (2002), Ingle et al. (2002b), Kieffer et al. (2002), and Weis and Frey (2002). **A.** Kerguelen Plateau samples inferred to contain a continental crust component. Samples from Sites 738 and 1137 show a pronounced depletion in Nb and Ta; the sample from Site 747 is relatively depleted in Nb, Ta, and Th; and the sample from Site 1136 is only slightly depleted in Nb and Th. **B.** Broken Ridge samples. The tholeiitic basalt forming Unit 6 at Site 1142 is relatively depleted in Sr, Nb, and Ta; the deficiency in Nb-Ta is inferred to indicate a component derived from continental crust. In contrast, the alkalic basalt at Sites 1141 (Unit 4) and 1142 (Unit 1) are relatively enriched in Nb and Ta but highly depleted in Th; this Th deficiency is inferred to be a characteristic of the Kerguelen plume (Neal et al., 2002). **C.** Southern Kerguelen Plateau samples that have relative abundances similar to primitive mantle. They contain no evidence for a continental component, and they have relatively high $^{143}Nd/^{144}Nd$ (Fig. **F8,** p. 45). **D.** Northern Kerguelen Plateau samples from Site 1140. Like mid-ocean-ridge basalt (MORB), samples from Units 1, 3, and 5 are relatively depleted in the most incompatible elements. These samples also have MORB-like Sr and Nd isotopic ratios (Fig. **F8,** p. 45). In contrast, samples from Units 2 and 3 are relatively enriched in the most incompatible elements and they contain a plume component. All samples from Site 1140 lack a relative depletion in Nb and Ta (i.e., there is no evidence for a continental component), but relative depletion in Sr (Units 2 and 3) reflects fractionation of plagioclase, which is present as a phenocryst. **E.** Typical tholeiitic basalt from Site 1138 (CKP) contrasted with trachybasalt from Site 1139 (NKP). The alkalic lavas at Site 1139 are the most incompatible element-rich lavas recovered from the Cretaceous LIP. Their Sr deficiency reflects plagioclase fractionation and the deficiency in Th, Nb, and Ta (similar to data for Site 747 in panel A may reflect a lower continental crust component. Kieffer et al. (2002) consider this interpretation, but they note that the plume source may be deficient in Th. A Th depletion also characterizes the alkalic basalt at Sites 1141 and 1142 (panel B), and Neal et al. (2002) infer that Th depletion is a source feature. N-MORB = normal mid-ocean-ridge basalt. (**Figure shown on next page.**)

Figure F7 (continued). (Caption shown on previous page.)

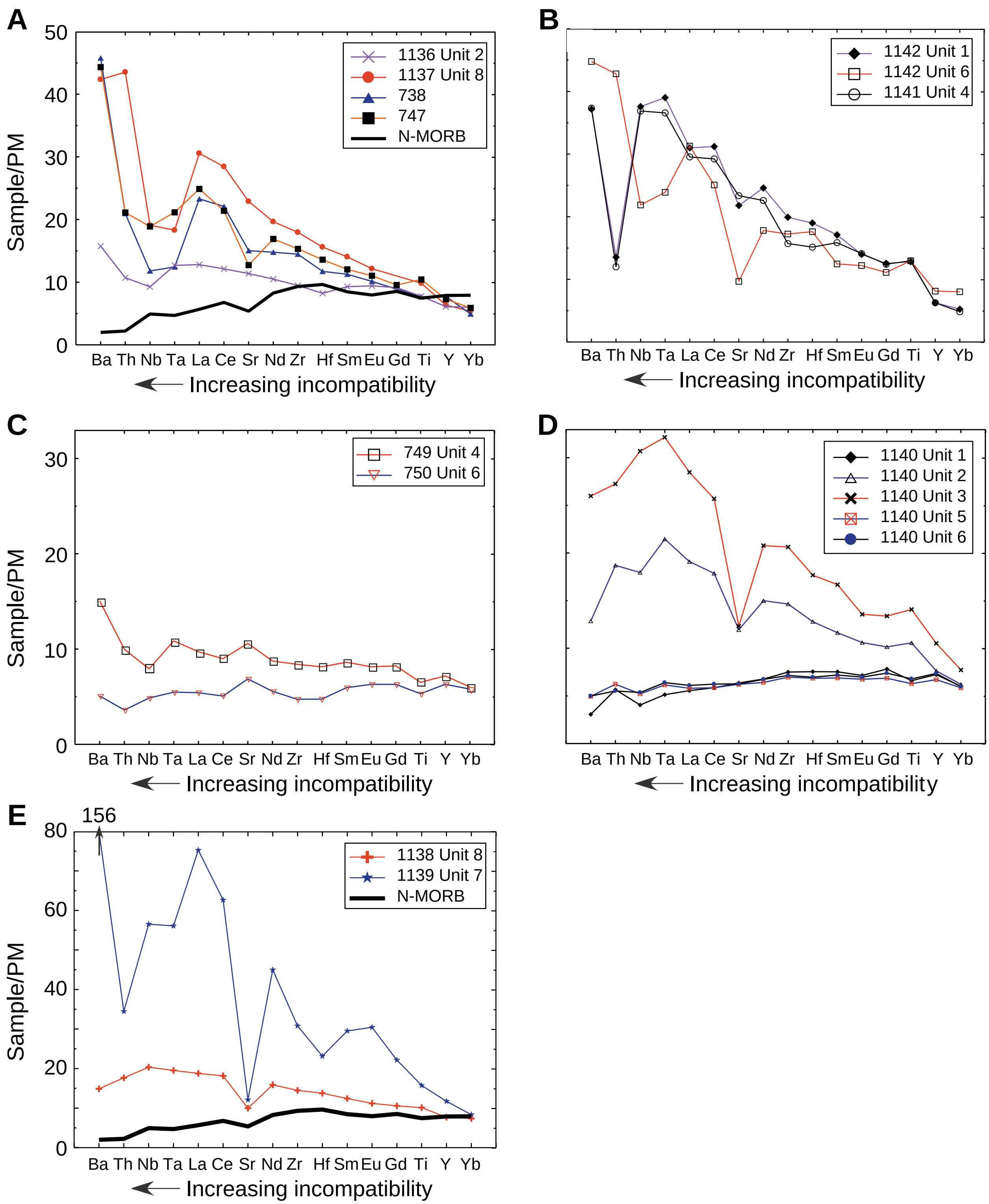

Figure F8. $^{143}Nd/^{144}Nd$ vs. $^{87}Sr/^{86}Sr$ for mafic rocks, dominantly tholeiitic basalt, except for alkalic basalt from Sites 1139, 1141, and 1142, recovered by drilling the igneous basement of the Kerguelen Plateau and Broken Ridge. All data are corrected to the time of eruption using measured parent/daughter abundances and ages from Duncan (2002) and Nicolaysen et al. (2000). Data sources are Site 738 (Mahoney et al., 1995), Sites 747, 749, and 750 (Frey et al., 2002b), Sites 1136, 1138, 1141, and 1142 (Neal et al., 2002), Site 1137 (Weis et al., 2001; Ingle et al.; 2002b), Site 1139 (Kieffer et al., 2002, only data for mafic lavas are plotted), and Site 1140 (Weis and Frey, 2002). The five data points with a black "x" within the symbol indicate unpublished data of D. Weis for geochemical reference samples selected to assess interlaboratory differences (one from Site 1136, two from Site 1138, and two from Sites 1141/1142). The results demonstrate the agreement of isotopic ratios for acid-leached samples obtained in the laboratories of D. Weis (Université Libre de Bruxelles) and J. Mahoney (University of Hawaii). The distinctive Unit 3 basalt at Site 1136 is labeled. Shown for comparison are fields for recent Southeast Indian Ridge (SEIR) mid-ocean-ridge basalt (MORB) (Mahoney et al., 2002) and the Cenozoic (24–30 Ma) flood basalt forming the Kerguelen archipelago (data sources are Yang et al., 1998; Doucet et al., 2002; Frey et al., 2000b, 2002a; D. Weis, unpubl. data). N-MORB and E-MORB = normal and enriched MORB, respectively. Important features are (a) lavas from most of the basement sites in the LIP define distinct fields with inverse correlation between $^{143}Nd/^{144}Nd$ and $^{87}Sr/^{86}Sr$; the greatest scatter from an inverse trend is for the highly altered mafic lavas from Site 1139. (b) A large proportion of the data for LIP samples either overlap with the field for the Kerguelen archipelago or are offset to lower $^{143}Nd/^{144}Nd$ and $^{87}Sr/^{86}Sr$. The offset of data for Sites 749, 1136, 1138, 1137, and 747 to lower ratios may reflect the eruption age differences (i.e., radiogenic ingrowth in the source from ~120 to 100 Ma for the plateau to ~25 to 30 Ma for the archipelago). For example, the arrow emanating from a Site 1138 data point shows the increase in $^{143}Nd/^{144}Nd$ and $^{87}Sr/^{86}Sr$ arising from 80 m.y. of ingrowth of a source with $^{147}Sm/^{144}Nd = 0.20$ and $^{87}Rb/^{86}Sr = 0.06$. These parent/daughter ratios are constrained by requiring that $(Sm/Nd)_{source} > (Sm/Nd)_{basalt}$ and $(Rb/Sr)_{source} < (Rb/Sr)_{basalt}$. (c) Samples from Site 1140 are consistent with mixing between components related to SEIR MORB and the Kerguelen plume (e.g., Weis and Frey, 2002). (d) The extreme values for Site 738 have been interpreted as reflecting a component derived from continental lithosphere, probably crust (Mahoney et al., 1995). (e) Although not as obvious, the trends to relatively high $^{87}Sr/^{86}Sr$ at relatively low $^{143}Nd/^{144}Nd$ defined by basalt from Sites 1137 and 747 have also been attributed to a component derived from continental crust (Weis et al., 2001; Frey et al., 2002b; Ingle et al., 2002b).

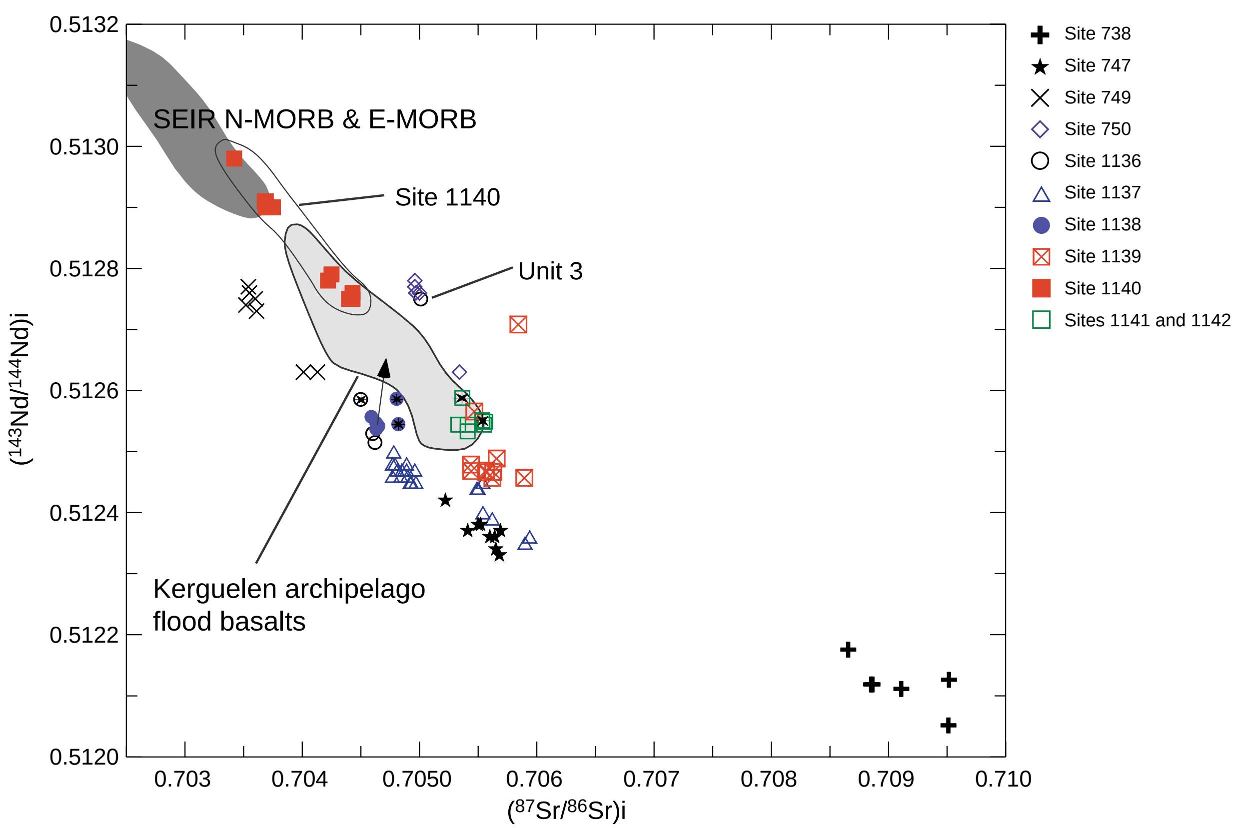

Figure F9. A, B. $^{207}Pb/^{204}Pb$ and $^{208}Pb/^{204}Pb$ vs. $^{206}Pb/^{204}Pb$ for mafic rocks, dominantly tholeiitic basalt recovered by drilling the igneous basement of the Kerguelen Plateau and Broken Ridge. Also shown is a field for the clasts of continental material in the conglomerate at Site 1137 (Ingle et al., 2002a). The anomalous Unit 3 at Site 1136 and Unit 6 at Site 1142 are labeled. There are four points with a black "x" within the symbol, one each for Sites 1136 and 1138 and two for Sites 1141/1142 including the anomalous Unit 6 at Site 1142. These points indicate unpublished data of D. Weis for geochemical reference samples selected to assess interlaboratory differences. The results demonstrate the agreement of isotopic ratios for acid-leached samples obtained in the laboratories of D. Weis (Université Libre de Bruxelles) and J. Mahoney (University of Hawaii). Because U-Th-Pb abundance data are not available for all samples, the data are not age corrected; however, the major features of the plots are not significantly affected by age correction (e.g., see table 2 of Neal et al., 2002). Data sources are Site 738 (Mahoney et al., 1995), Sites 747, 749, and 750 (Frey et al., 2002b), Sites 1136, 1138, 1141, and 1142 (Neal et al., 2002), Site 1137 (Weis et al., 2001; Ingle et al., 2002b), Site 1139 (Kieffer et al., 2002, only data for mafic lavas are plotted), and Site 1140 (Weis and Frey, 2002). Shown for comparison are fields for recent Southeast Indian Ridge (SEIR) mid-ocean-ridge basalt (MORB) and the Cenozoic (24–30 Ma) flood basalt forming the Kerguelen archipelago (data sources are Yang et al., 1998; Doucet et al., 2002; Frey et al., 2000b, 2002a; D. Weis, unpubl. data). N-MORB and E-MORB = normal and enriched MORB, respectively. Important features are (a) the relatively young (34 Ma) Site 1140 basaltic samples define a mixing trend between the fields for the Kerguelen archipelago and SEIR MORB (Weis and Frey, 2002). (b) Relative to the Kerguelen archipelago field, the Cretaceous LIP samples are offset to low $^{206}Pb/^{204}Pb$. Aging of the source for 80 to 95 m.y. with $^{238}U/^{204}Pb = 10$, a reasonable maximum, increases $^{206}Pb/^{204}Pb$ by <0.15; hence, the lower $^{206}Pb/^{204}Pb$ of the plateau lavas relative to the archipelago lavas cannot be explained by radiogenic ingrowth. Three sites (747, 750, and 1139) have lavas with very low $^{206}Pb/^{204}Pb$, <17.8; in the $^{207}Pb/^{204}Pb$ vs. $^{206}Pb/^{204}Pb$ plot, data for these sites define a steeper trend than that of the MORB field. (c) When grouped together, a near-vertical trend of increasing $^{207}Pb/^{204}Pb$ and $^{208}Pb/^{204}Pb$ at a moderate $^{206}Pb/^{204}Pb$ of ~18 is defined by lavas from Sites 749 < 1138 < 1136 < 1141/1142 and 1137. Site 738 basalt also has high $^{207}Pb/^{204}Pb$ and $^{208}Pb/^{204}Pb$ but at a slightly lower $^{206}Pb/^{204}Pb$.

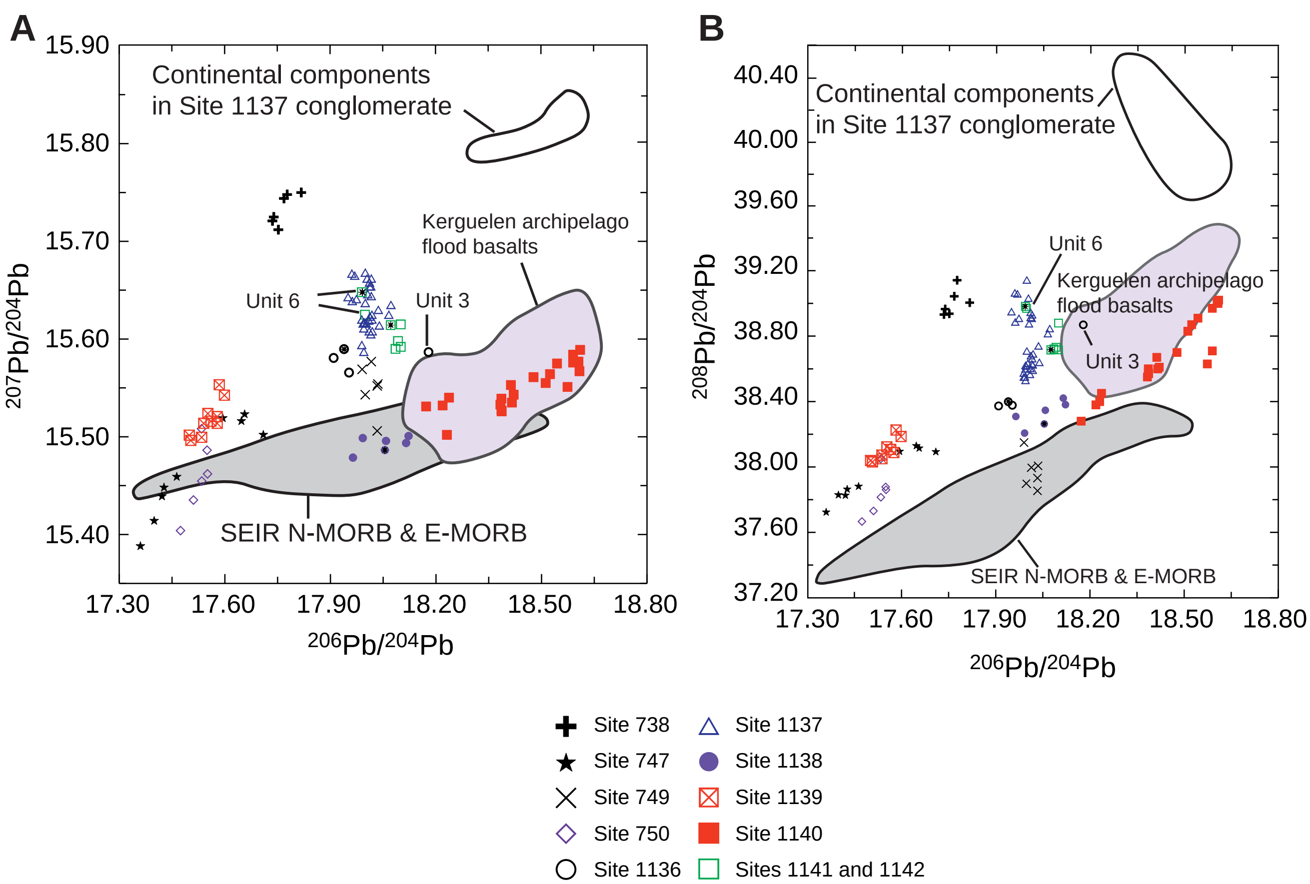

Figure F10. Δ8/4 vs. $(La/Nb)_{PM}$. Δ8/4 is a measure of the vertical distance of data points in Figure F9B, p. 46, from the Northern Hemisphere Reference Line of Hart (1984). Subscript "PM" indicates normalized to the primitive mantle estimate of Sun and McDonough (1989). Continental crust is characterized by high Δ8/4 and $(La/Nb)_{PM}$. Data sources are Site 738 (Mahoney et al., 1995), Sites 747, 749, and 750 (Frey et al., 2002b), Sites 1136, 1138, 1141, and 1142 (Neal et al., 2002), Site 1137 (Weis et al., 2001; Ingle et al.; 2002b), Site 1139 (Kieffer et al., 2002, only data for mafic lavas are plotted), and Site 1140 (Weis and Frey, 2002). Also plotted are data for dredged basalt from Broken Ridge (Mahoney et al., 1995). Important features are (a) emanating from the field defined by Kerguelen archipelago flood basalt, samples from Site 1139, Site 1137, Unit 6 of Site 1142, Site 738, and dredges from eastern Broken Ridge (BR) define a positive trend. The highest values, data for lavas from eastern Broken Ridge, Sites 738 and 1137, are interpreted to reflect a component derived from continental crust (Mahoney et al., 1995; Weis et al., 2001; Ingle et al., 2002b). Note that such a component is absent from Cenozoic basalt at Site 1140 and the flood basalt of the Kerguelen archipelago. (b) Data for two sites, 749 and 1140, have low Δ8/4, and data for three sites deviate from the positive trend; that is data for Sites 1141 and 1142 (except Unit 6) have moderately high Δ8/4 but $(La/Nb)_{PM} < 1$, and data for Site 747 define a horizontal trend with moderate Δ8/4 but $(La/Nb)_{PM} > 1$.

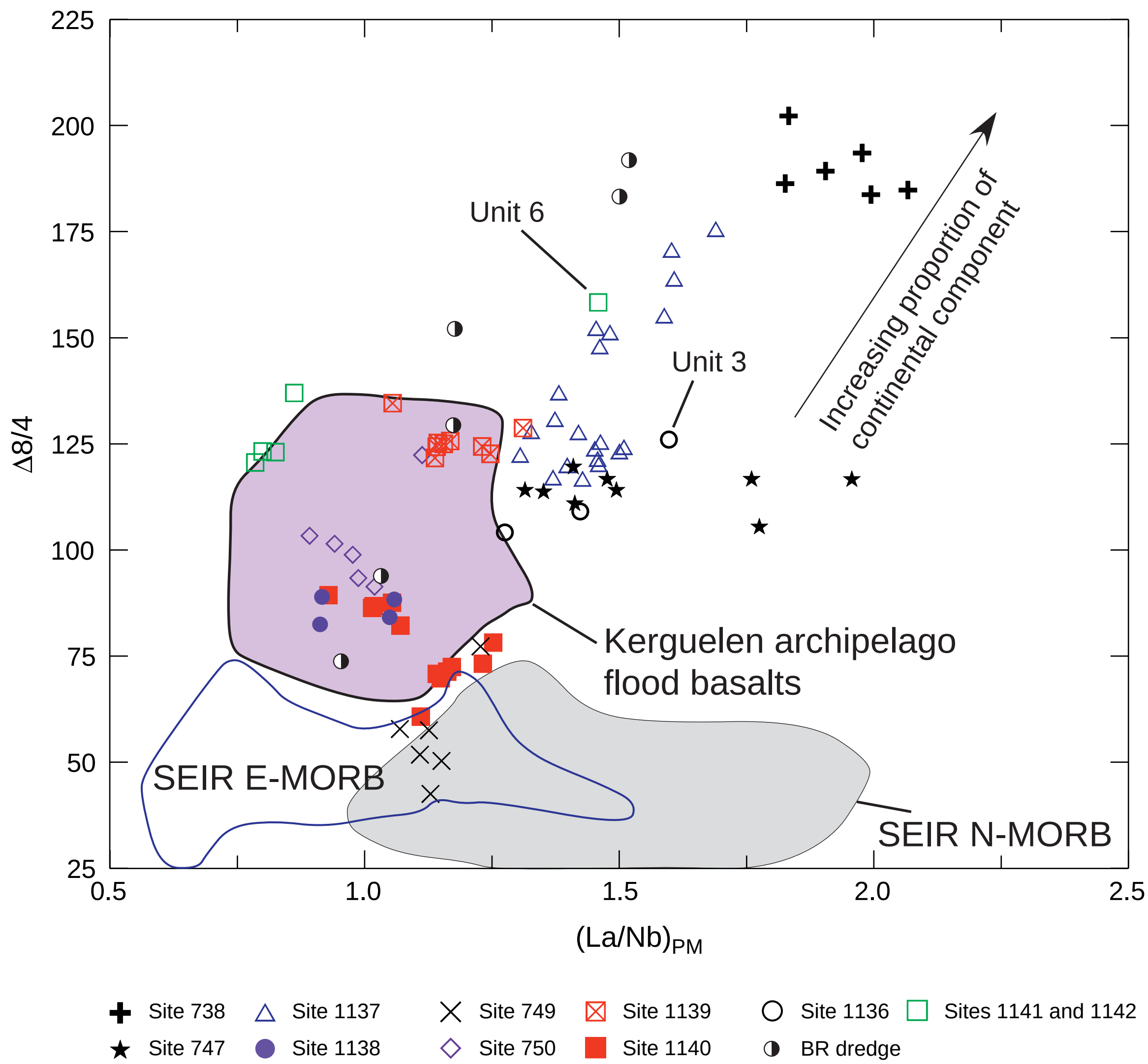

Figure F11. Subsidence estimates for various parts of the Kerguelen Plateau plotted as a function of eruption age of basement basalts (from Wallace, 2002). The subsidence for Site 1140 is calculated using H_2O and CO_2 data for glassy pillow rims. For all other sites, the basement basalts were erupted in a subaerial environment, so there is no information on the original elevation above sea level at the time of eruption. Therefore, to estimate subsidence, we have assumed that (1) these other sites subsided like normal Indian Ocean lithosphere from the time of eruption until the time represented by the oldest marine sediments on top of basement, and (2) at the time of the oldest marine sediment, the site was at sea level. Note that assumption 1 only affects the first 10–35 m.y. following the initiation of subsidence. For each site, subsidence from the time of the oldest marine sediment to the present day is shown as a thin blue line. For reference, the heavy solid line shows the subsidence curve for normal Indian Ocean lithosphere (Hayes, 1988). Eruption ages were determined by $^{40}Ar/^{39}Ar$ dating (Duncan, 2002; Pringle et al., 1994). Biostratigraphic ages are from Coffin, Frey, Wallace, et al. (2000) and references therein. For all sites, including Site 1140, the present-day depth of the top of igneous basement has been corrected for sediment loading (i.e., the actual present-day depth is greater than would have occurred due to thermal subsidence alone because of the additional effect of sediment loading). The corrected basement depth (D_c) is obtained from the equation of Crough (1983): $D_c = d_w + t_s (\rho_s - \rho_m)/(\rho_w - \rho_m)$, in which d_w = water depth in meters, t_s = sediment thickness in meters, ρ_s = average sediment density (1.90 g/cm^3), ρ_m = upper mantle density (3.22 g/cm^3), and ρ_w = seawater density (1.03 g/cm^3). Error bars show uncertainty in the subsidence estimates. For Site 1140, this uncertainty is based on uncertainty of the original eruption depth due to variations in the H_2O and CO_2 data for glassy pillow rims. For all other sites, error bars show an estimate of the combined uncertainties resulting from assumptions 1 and 2 above and the correction for effects of sediment loading on subsidence.